GnRH-1 Neurons Are Not in the Goofy Group: 123cre Tracing Sets the Record Straight

Enrico Amato Jr., Mia V. Call, Noah M. LeFever, Mya Aviles-Carlos, Nikki M. Dolphin, Paolo E. Forni

Department of Biological Sciences, The Center for Neuroscience Research, The RNA Institute, University at Albany, State University of New York, Albany, New York, USA.

*Corresponding author: pforni@albany.edu

Abstract

The olfactory placode (OP) gives rise to a wide array of chemosensory neurons in the nasal region, including olfactory sensory neurons, vomeronasal sensory neurons, and those of the septal organ and Grueneberg ganglion. During placodal invagination, the OP also produces several classes of migratory neurons, such as gonadotropin-releasing hormone-1 (GnRH-1) neurons, terminal nerve (TN) neurons, and olfactory pioneer neurons, the latter of which are thought to play a key role in initiating olfactory bulb development. Despite decades of research, the genetic lineage and molecular identity of the various neuronal types that arise from the OP remain under investigation. The GnRH-1 neurons play essential roles in reproduction as well as chemodetection; however, they appear to have a distinct genetic lineage from olfactory and vomeronasal chemosensory neurons. The Golgi-associated olfactory signaling regulator (Goofy/Gfy) is known to be expressed in developing chemosensory neurons. To determine whether the expression of this gene is specific to the neurons of the nasal chemosensory epithelia or a common feature of OP derivatives, we characterized its expression and lineage at both embryonic and postnatal stages. Our results confirm broad expression across developing chemosensory neurons and by subsets of olfactory pioneer neurons. However, our data show that the GnRH-1 neurons do not express Gfy and suggest only sparse expression across the putative TN neurons. These findings highlight a previously unknown genetic distinction between

neuronal populations of the nasal migratory mass and the chemosensory populations in the nasal region.

Introduction

The olfactory placode (OP) is the ectodermal thickening responsible for the development of the olfactory system of vertebrates (Verwoerd and van Oostrom, 1979). In mice, the OP primordium can first be identified at E9.0 (embryonic day 9) (Ikeda et al., 2007; Klein and Graziadei, 1983; Rawson, 1999). The OP then invaginates around E10.5 (Brunjes and Frazier, 1986; Tarozzo et al., 1995) to give rise to the olfactory pit which further develops into multiple derivatives which include various specialized chemosensory epithelia: the main olfactory epithelium (OE), the vomeronasal organ (VNO), septal organ and Gruenberg ganglion (GG) (Couly and Le Douarin, 1985; Cuschieri and Bannister, 1975b). As the OP forms and then invaginates, it undergoes several waves of neurogenesis (Forni et al., 2013; Paronett et al., 2023; Rukh et al., 2024). Around E10.5, shortly after its formation, the OP is highly proliferative, and presents mitotic figures in the apical layers (Cuschieri and Bannister, 1975a; Graham et al., 2007; Smart, 1971; Taroc et al., 2020)

Between E10.5 and E11.5 the OP mostly produces migratory neurons that leave the OP and migrate toward the developing brain (Fornaro et al., 2003; Forni et al., 2011a; Murakami et al., 2022). The migratory neurons include the gonadotropin-releasing hormone-1 (GnRH-1) neurons, presumptive terminal nerve (TN), and the presumptive olfactory pioneer neurons, which are crucial for inducing olfactory bulb (OB) formation (Gong and Shipley, 1995). Around E11, the number of Achaete-scute homolog-1 (Ascl1)-expressing neuronal progenitors increases in the developing olfactory epithelia, and the neurogenesis of most chemosensory neurons is established (Guillemot et al., 1993; Taroc et al., 2020).

The GnRH-1 neurons are broadly accepted to have a placodal origin in vertebrates (Murakami et al., 2022; Schwanzel-Fukuda and Pfaff, 1989; Whitlock and Westerfield,

2000; Wray et al., 1989). The GnRH-1 neurons are ancestral cells (Herbison, 2025), in fact, both GnRH peptides and GnRH-expressing neurons have been reported in ascidians, where specialized olfactory chemosensory epithelia are absent and only proto-placodal structures have also been described (Abitua et al., 2015; Kamiya et al., 2014; Poncelet and Shimeld, 2020; Sakai et al., 2020; Stolfi et al., 2015).

The TN neurons form the migratory mass, along with the olfactory pioneer neurons, neuropeptide-Y (Npy) expressing neurons, Somatostatin (Sst) expressing neurons, the GnRH-1 neurons, and the olfactory ensheathing cells (Demski and Schwanzel-Fukuda, 1987; Hilal et al., 1996; Miller et al., 2010; Murakami et al., 2022; Taroc et al., 2017; Valverde et al., 1993; Vilensky, 2012).

The migratory neurons emerging from the developing olfactory structures exhibit several molecular/genetic differences relative to the chemosensory neurons of the olfactory and vomeronasal epithelia. The GnRH-1 neurons express the transcription factor Isl1, which defines a unique genetic lineage across the neurons of the migratory mass (Lund et al., 2020; Shan et al., 2020; Taroc et al., 2020). Additionally, the GnRH-1 neurons can form in animals with loss-of-function mutations in the transcription factor Gli3, which instead causes severe impairment of olfactory and vomeronasal neurogenesis (Taroc et al., 2020). Furthermore, characterization of mice expressing the human Peripherin BAC transgene or Prokineticin Receptor 2-Cre (Prokr2Cre) suggests distinct genetic lineages between the migratory pioneer-TN neurons and the GnRH-1 neurons (Amato et al., 2024; Taroc et al., 2017).

GnRH-1, TN, and olfactory pioneer neurons are among the earliest neuronal populations to develop in the nose. Prokr2Cre lineage tracing showed that these cells can be identified genetically and through strong immunoreactivity for Cntn2 (TAG-1) and Map2 between E11.5 and E14.5. In contrast, little to no immunoreactivity for either marker is seen in the sensory neurons of the developing olfactory and vomeronasal epithelia (Amato et al., 2025; Schwarting et al., 2001; Taroc et al., 2017).

Patients affected by Kallmann syndrome are characterized by a defective sense of smell and delayed or absent puberty (Forni and Wray, 2015; Kallmann, 1944; Lieblich et al.,

1982). Roles of GnRH-expressing neurons for chemodetection have been proposed from ascidians to vertebrates (Abitua et al., 2015; Umatani and Oka, 2019). Recent data have identified that a subpopulation of GnRH-1 neurons around the OB plays a role in processing chemosensory signals (Decoster et al., 2024). Notably, this group of OB GnRH-1 neurons has been shown to function in both mating behavior and in olfactory preference for opposite-sex odors. These data indicate that GnRH-1 neurons, beyond their established function in regulating the hypothalamic-pituitary-gonadal axis, can also play a crucial role in processing chemosensory stimuli (Umatani and Oka, 2019).

The developmental relationship between the olfactory system and the other neurons of the migratory mass has been a matter of investigation for decades. However, the lack of distinct markers and defined genetic entry points has hindered efforts to identify early nasal neurons and clarify the functions of specific genes in their development. The Golgi Associated Olfactory Signaling Regulator (Goofy/ Gfy) is an integral membrane protein located in the Golgi membrane, which is expressed in nasal chemosensory neurons of rodents, including neurons of the main olfactory epithelium (OE), vomeronasal sensory epithelium (VSE), and GG (Kaneko-Goto et al., 2013). Here, we characterized Gfy expression and genetic lineage during early stages of olfactory development (E11.5-E15.5) and the postnatal VNO. Our data indicates a molecular distinction and differences in developmental dynamics between the migratory neuronal population originating from the OP and the neurons belonging to the specialized chemosensory system of rodents.

Results

Gfy is heterogeneously expressed across newly formed neurons in the developing olfactory system

The developing OP and its derivatives are highly neurogenic, resulting in continuous and asynchronous neuronal production throughout the nasal region. In mouse, neurogenesis in the OP starts soon after its formation around E9.5, as pioneer neurons can be already detected at E10.5 (Chen et al., 2009; Fornaro et al., 2003; Forni et al., 2011b;

117 Katoh et al., 2011). Analyzing single-cell RNA sequencing data of the nasal area at E14.5
118 (Fig. 1A) (Amato et al., 2024), we found Gfy expression in cell clusters containing the
119 olfactory maturation marker gene Omp (Olfactory marker protein) expressing putative
120 developing chemosensory neurons (OSNs/VSNs), as well as in some of the putative
121 migratory pioneer/TN neurons (positive for Prokr2) (Amato et al., 2024) (Fig. 1F,H,I). By
122 analyzing Gfy expression (Fig. 1A-I) and its correlation (Fig. 1J) with markers of
123 neurogenesis and olfactory maturation, we found that Gfy is not expressed by proliferative
124 olfactory-vomeronasal progenitors (Ascl1+) (Fig. 1B), nor by olfactory-vomeronasal
125 precursors expressing Neurod1 and Neurog1 (Fig. 1C-D). However, its expression
126 correlates with the RNA binding protein Elav3 (HuC) (Fig. 1E) and reaches its highest
127 correlation with Gap43 (Growth Associated Protein 43), a neuron-specific protein
128 expressed during axon growth (Karns et al., 1987; Verhaagen et al., 1989) (Fig. 1G, J). Gfy
129 expression is further retained in cells expressing mRNA of Omp (Fig. 1G-J). These data
130 support Gfy expression across various postmitotic maturing neurons originating from the
131 OP (Kaneko-Goto et al., 2013; Margolis, 1972; Margolis and Tarnoff, 1973).
132
133 **The GfyCre (123Cre) mouse line can produce different recombination patterns; in**
134 **chemosensory epithelia recombination starts to be apparent at E12**
135 To further characterize the Gfy genetic lineage across the various neurons
136 originating from the OP, we bred GfyCre mice with homozygous R26tdTomato (Ai14$^{-/-}$)
137 reporter mice. PCR analysis of the pups showed Cre inheritance following the expected
138 Mendelian ratios (data not shown); however (Fig. S1A-C), among the Cre-positive pups, we
139 observed two recombination patterns: 1) a highly chimeric recombination throughout the
140 body, including the chemosensory epithelia, and 2) recombination limited to the
141 chemosensory regions of the developing nose. Notably, similar recombination patterns
142 were seen regardless of whether the Cre was inherited maternally or paternally. From this
143 point on, we will discuss only results from animals in which recombination is limited to the
144 nasal chemosensory epithelia.

145 We examined embryos at multiple stages from E11.5 to E15.5 (Fig. 2). At E11.5, only
146 a few neurons positive for recombination were observed, some of which appeared in the
147 developing OE and VNO, whereas others were seen in the nasal mesenchyme (Fig. 2A). At
148 E12.5 and E13.5, neurons positive for recombination were clearly detected in the
149 developing chemosensory epithelia and in migratory neurons associated with Peripherin-
150 positive fibers (Fig. 2B-C). By E14.5 and E15.5, widespread recombination was evident
151 across the olfactory-vomeronasal epithelia and their projections to the OB (Fig. 2D-E), as
152 well as in neurons of the Gruenberg ganglion (GG) (Fig. S2) (Kaneko-Goto et al., 2013).
153 Notably, at these stages, we also observed Peripherin-positive fibers resembling those of
154 the putative TN invading the brain ventrally to the OB, which appeared negative for
155 recombination (Fig. 2D-E). The migratory neurons forming within the OP are readily
156 detectable at E10.5 (Fornaro et al., 2003; Forni et al., 2011b; Miller et al., 2010), prior to the
157 initial neurogenesis of the olfactory/vomeronasal chemosensory neurons that begins
158 around E11.5 (Rawson et al., 2010; Taroc et al., 2020). Around 2-3 days after the beginning
159 of neurogenesis in the OP (E11.5 and E12.5), the vomeronasal epithelium and part of the
160 migratory mass showed only sparse GfyCre recombination(Fig. 2A-B).
161 To better determine the time reference between the birth of chemosensory neurons
162 and GfyCre recombination, we injected GfyCre$^{+/-}$/A14$^{-/-}$ embryos with EdU first at E10.5,
163 then again at E11.5, and analyzed them at E14.5. (Fig. 3A). At this stage, we found that only
164 ~60% (SD ± 3.02) of EdU-positive neurons born 3 or 4 days before showed detectable
165 recombination (Fig. 3B-E). Altogether, this indicates that GfyCre-mediated recombination
166 is variably detected between 2 and 4 days after neurogenesis.
167
168 **Gfy is neither expressed by the GnRH-1 neurons nor by other neurons migrating from**
169 **the nose to the brain.**
170 After confirming that GfyCre mice exhibited the expected recombination in
171 chemosensory neurons within 3 days from neurogenesis, we aimed to understand if the
172 Gfy lineage included ancestral cells such as the TN neurons, GnRH-1 neurons, or other
173 neuronal populations that form in the nose and migrate to the brain (Hilal et al., 1996;

Murakami et al., 2022; Murakami et al., 2024). The GnRH-1 neurons form between E10 and E12 (Jasoni et al., 2009; Schwanzel-Fukuda and Pfaff, 1989; Wray et al., 1989). To trace different neurogenic waves of the GnRH-1 neurons in GfyCre/Ai14 embryos, some dams were injected with EdU at E8.5 and E9.5, and others at E10.5 and E11.5 (Fig. S3). We found that 15% (SD ± 5.35) of the GnRH-1 neurons were labeled by EdU injection at E8.5 and E9.5 (Fig. S3B-C''), while 40% (SD ± 7.59) were labeled after injections at E10.5 and E11.5 (Fig. S3D-F''). Notably, at all analyzed stages (E11.5 to E15.5) we never found GnRH-1 neurons or other neuronal cells positive for Gfy tracing in the brain (Fig. 4), suggesting that Gfy is not expressed in newly formed or maturing GnRH-1 neurons even 6 days after neurogenesis. However, EdU injections at E10.5 and E11.5 revealed that 50% (SD ± 2.97) of migratory Gfy traced neurons in the nose were labelled with EdU at these stages (Fig. S4) (Change images for Fig. S4).

The terminal nerve neurons are negative for GfyCre tracing

In a recent paper, Prokr2 was identified as a reliable genetic marker for the neurons forming the TN as well as for putative olfactory pioneer neurons. In the developing nose, migratory cells positive for Prokr2Cre/Ai14 tracing can also be identified based on high immunoreactivity for Map2 up to E14.5 (Amato et al., 2024). However, by pairing GfyCre tracing with Map2 immunostaining at E14.5, we found that only a subset of Map2-positive migratory neurons were also positive for GfyCre tracing (Fig. 5A-B'').

In line with work done in chick (Murakami et al., 2022), we observed that also in mouse, cells expressing Sst emerge from the developing VNO and appear to migrate as part of the migratory mass toward the brain, however, Sst expressing cells were not positive for Gfy tracing (Fig. 5C-E). In contrast, by using Prokr2Cre tracing, we observed that Sst is expressed at least transiently by some of the Prokr2 traced migratory cells (Fig. 5F-H''). In Prokr2 traced animals immunolabelled against Sst, we found that some of the Sst expressing cells, were also positive for Prokr2 tracing in the migratory mass. However, Sst expressing cells in the brain appeared to be negative for both GfyCre and Prokr2Cre tracing. (Fig. 5H-H'').

203 Analyzing GnRH-1 migration (Fig. 4D), we could see that the GnRH-1 neurons invading
204 the brain, were not associated with GfyCre traced fibers. In fact, the Peripherin+ fibers of the
205 TN appeared negative for Gfy tracing (Fig. 2), though sparse axons positive for Gfy tracing
206 could be found in the basal forebrain (Fig. S5B-B'').
207 To determine whether Gfy-tracing could discriminate among different subpopulations of
208 Map2–Prokr2–expressing migratory neurons, we compared E14.5 GfyCre and Prokr2Cre
209 lineage-traced embryos (Fig.5I-I''). In Prokr2Cre-traced animals, neuronal cell bodies and
210 fibers extended into the brain alongside the migrating GnRH-1 neurons. In contrast, GfyCre
211 tracing labeled only neurons that remained within the nasal region. No GfyCre traced cell
212 bodies enter the forebrain (Fig. 2, 4). These results suggest that while the migratory neurons
213 expressing Prokr2, GnRH-1, and Sst invade the brain, the cell bodies belonging to the GfyCre
214 lineage remain in the nose.
215
216
217 **Following Gfy expression in postnatal VSNs revealed differences in the developmental**
218 **dynamics of V1R and V2R VSNs.**
219 The expression of Gfy in newly generated neurons makes this line a valuable tool for
220 manipulating chemosensory neurons prior to their maturation. Because of our focus on
221 neuronal populations of and arising from the vomeronasal primordium, we further
222 examined Gfy expression in this area. During embryonic development, we found that
223 GfyCre recombined in both Meis2 and AP-2ε (Tfap2e) expressing neurons, which later will
224 mature into V1R and V2R VSNs respectively (Fig. S6) (Enomoto et al., 2011; Katreddi et al.,
225 2022).
226 To characterize GfyCre recombination in relation to postnatal vomeronasal
227 neurogenesis, we reanalyzed whole-VNO single cell RNA-sequencing datasets (Hills et al.,
228 2024; LeFever et al., 2024) and reconstructed the canonical dichotomy of apical and basal
229 VSN development (Fig. 6A). UMAP projections and expression overlays for progenitors
230 (Ascl1, Mki67, Neurog1), precursors (non-proliferative Neurog1, Neurod1), maturing VSNs
231 (Gap43, Gng8/Gy8 and Gfy) and the maturation marker Omp. These recapitulated the

expected neurogenic sequence, with progenitors at the base of the Y-trajectory, transitioning through neuronal precursors and immature VSNs, and diverging into the apical and basal branches, which culminate in mature V1R/Meis2+ and V2R/AP-2ε+ neurons (Fig. 6B).

Pearson coefficient calculation of global gene–gene correlation revealed consistent transcriptional changes across the dataset (Fig. 6C). This analysis showed that in contrast to what was observed during embryonic development (Fig. 1J), a negative correlation between Gfy and Gap43, along with a positive correlation between Gng8 and Omp. This suggests that postnatally, Gfy is expressed with a delay relative to Gap43 in maturing neurons and maintains high expression in mature neurons, while Gng8 clusters with intermediate neuronal states (Fig. 6D,G).

When the apical and basal branches were examined separately, we found additional interesting differences in their internal development (Fig. 6E–E"). In fact, we noticed that Gap43 expression rises earlier in Meis2+/apical lineage as opposed to AP-2ε+/basal lineage (Fig. 6E', E''). On the contrary, the Meis2-/basal lineage was found to have a negative correlation between Neurod1 and Gap43.

Further analysis at precursor stages reinforced this difference (Fig. S7), showing higher Gap43 and Gfy expression in the Meis2+/apical lineage. Moreover, by performing correlation analysis on Meis2+/apical and AP-2ε+/basal precursor populations, we observed that Meis2+ cells have a more precocious expression of Gfy, partial overlapping with Neurod1 and Omp (Fig. S7C'-C''). Suggestive of differences in developmental dynamics between the two main types of VSNs.

From previous work we know that V2R VSN specific transcription factor Ap2e directly binds and negatively regulates the expression of the Gt(ROSA)26Sor locus (Lin et al., 2022). Based on that, we assessed expression of the Gt(ROSA)26Sor locus to evaluate baseline reporter activity across VSN classes. Violin plots revealed a modest but consistent elevation in ROSA expression in apical (Meis2+) VSNs relative to basal neurons (AP-2ε+) (Fig. 6F), suggesting lineage-specific differences that may influence reporter sensitivity in genetic tracing experiments.

To validate some of these observations in vivo, we combined GfyCre lineage tracing with Gap43 immunofluorescence (Fig. 7A-A'''). At P30, GfyCre-traced neurons were present in both immature and mature VSNs. However, a difference in the intensity of tdTomato expression was visibly noticeable between neurons in the apical and basal territories (Fig 7A-A"). In the marginal zones, where the VSNs give rise to maturing Gap43+ cells, we noticed that tdTomato fluorescence was often absent or very low, confirming that GfyCre-mediated recombination lags behind Gap43 expression.

As expected from their known axonal guidance programs, V1R/Meis2+ VSNs (Neuropilin-2+) projected to the anterior AOB, whereas V2R/AP-2ε+ VSNs (Robo2+) projected to the posterior AOB. GfyCre-mediated recombination was detected in the axons targeting both AOB domains (Fig. 7B-B''). The reduced Rosa26 expression characteristic of basal VSNs again translated into visibly weaker tdTomato signals in the posterior AOB glomeruli compared to those in the anterior AOB glomeruli (Fig. 6F).

Discussion

The lineage and developmental relationship between olfactory sensory neurons (OSNs) and neurons of the migratory mass in the developing nose has been a subject of much speculation. Early observations showed that the GnRH-1 neurons emerge from the OP and migrate alongside olfactory axons toward the forebrain, suggesting that a caudal branch of the vomeronasal nerve might provide structural or molecular cues essential for GnRH-1 pathfinding to the basal forebrain (Hanchate et al., 2012; Schwanzel-Fukuda and Pfaff, 1989; Wierman et al., 2011; Wray et al., 1989). This idea was strengthened by findings in Kallmann syndrome (Kallmann, 1944), where anosmia frequently co-occurs with failed GnRH-1 neuronal migration, implying a shared developmental dependency (Schwarting et al., 2001; Yoshida et al., 1995). However, subsequent work has suggested that the association between OSNs and GnRH-1 neurons is less direct than initially assumed. Accumulating evidence indicates that populations of neurons distinct from OSNs and VSNs serve as the primary substrates guiding GnRH-1 neurons into the brain (Amato et al.,

290 2025; Amato et al., 2024; Murakami et al., 2024; Taroc et al., 2019; Taroc et al., 2020; Taroc
291 et al., 2017). This evolving understanding has shifted the field away from the long-held
292 assumption of a direct OSN/VSN-GnRH link and toward a model in which multiple
293 placode-derived neuronal lineages play specialized and non-redundant roles in GnRH-1
294 migration (Murakami et al., 2022).
295 Here, we present a characterization of the neuronal cell types within the developing
296 olfactory system that can be genetically traced through the use of Gfy(123)Cre.
297 Characterizing the mice, we observed that 50% of the Cre-positive mice exhibit some early
298 Gfy expression during development that can lead to chimeric recombination (Fig. S1). This
299 is an important caveat for designing genetic strategies with this line, we suggest keeping
300 these mice on a reporter line to monitor the recombination pattern. However, at least 50%
301 of the GfyCre mice have the expected olfactory recombination.
302 From the experiments shown here, we provide new evidence distinguishing GnRH-1
303 neurons and other TN neuron cells from the OSN, VSN and GG lineages. Initial analysis of
304 Gfy expression using E14.5 single-cell RNA sequencing data revealed that both
305 differentiated olfactory neurons and groups of migratory neurons in the nose exhibit Gfy
306 enrichment (Fig. 1). Moreover, these data showed that Gfy largely overlaps with Gap43
307 expression during embryonic development (Fig. 1J). Consistent with these transcriptomic
308 findings, examination of GfyCre$^{+/-}$;Ai14$^{+/-}$ traced embryos revealed a progressive increase in
309 Gfy lineage tracing between E11.0 and E15.5, spanning many OSNs, VSNs, and GG
310 neurons, as well as their projections to the developing OBs (Fig. 2, S2). In addition, we also
311 identified subsets of Gfy labeled cell bodies that appeared to be migrating away from the
312 chemosensory epithelia toward the developing OBs (Fig. 2B-C). These results indicate that
313 some of the migratory neurons express Gfy, supporting prior observations that Gfy
314 expression is associated with neuronal populations forming from or belonging to the nasal
315 chemosensory epithelia (Baker and Farbman, 1993; Habif et al., 2023; Hirata et al., 2006;
316 Kaneko-Goto et al., 2013; Valverde et al., 1993).
317

318 Recent work identified Sst expression in cells invading the brain with the GnRH-1
319 neurons (Murakami et al., 2022). We observed that Sst is expressed by some of the
320 Prokr2Cre traced neurons but not positive for GfyCre tracing (Fig. 5C-H'').However, recent
321 data in mouse suggests that the GnRH-1 neurons themselves can express Sst, making it
322 possible that previously identified Sst cells include subsets or maturing GnRH-1 neurons
323 (Zouaghi et al., 2025). No overlap between GnRH-1, Sst, and Gfy tracing was observed at
324 any point during the development or migration of the GnRH-1 neurons (Fig. 4,5).
325 Interestingly, GnRH-1 immunoreactivity appears days before the onset of GfyCre
326 recombination. In fact, while at E11.5 and E12.5, numerous neurons within the VNO and
327 nasal area were positive for GnRH-1, only sparse cells showed detectable Gfy lineage
328 tracing (Fig. 4A-B''').
329 Our birth-dating experiments indicate that chemosensory neurons in the OE and
330 VNO undergo Cre-mediated recombination between 3-4 days after neurogenesis (Fig. 3).
331 Birth dating of GnRH-1 neurons confirmed that GfyCre recombination is not detectable in
332 these cells even 6 days after their generation (Fig. S3).
333 We previously identified that Prokr2Cre tracing and Map2 strong immunoreactivity
334 overlap in migratory TN neurons emerging from the developing olfactory epithelia. Notably,
335 some Prokr2+ expressing neurons also express GnRH-1 (Amato et al., 2024).
336 Map2 immunostaining combined with GfyCre lineage tracing revealed that approximately
337 50% of the migratory neurons within the migratory mass were positive for Gfy tracing (Fig.
338 5A–D). These findings indicate that at least half of the neurons previously identified by
339 Prokr2 lineage tracing also express Gfy, consistent with the embryonic single-cell
340 transcriptomic data (Fig. 1). Together, these data suggest that Prokr2 exhibits broader
341 expression across migratory neuronal populations, including olfactory pioneer and TN
342 neurons, while GfyCre is limited only to pioneer neurons that remain in the nasal
343 compartment. The GnRH-1 neurons enter the brain along TN fibers, which are positive for
344 Cntn2 (Tag1), Peripherin and Prokr2Cre lineage (Amato et al., 2025; Schwarting et al., 2001;
345 Taroc et al., 2017). However, Peripherin-positive TN projections that invade the basal
346 forebrain together with the GnRH-1 neurons were for the most part negative for Gfy tracing

(Fig. 2, S5). GfyCre does not label the GnRH-1 neurons, nor other cell bodies that invade the brain.

Following Gfy expression and recombination in the VNO lead us to some other interesting findings. GfyCre recombination occurs in neurons of both apical (Meis2/V1R) and basal (AP-2ε/V2R) vomeronasal lineages, indicating that Gfy is not lineage-restricted (Fig. 6). However, reanalysis of postnatal single-cell transcriptomic data of apical and basal trajectories reveals subtle but important differences in their maturation dynamics. Apical VSNs display earlier and stronger overlap between Gap43 and Gfy expression, whereas basal VSNs show delayed or weaker expression suggesting lineage-specific developmental gene expression progressions (Fig. 6E-E'') (Hills et al., 2024; Lin et al., 2018). These intrinsic differences extend to reporter sensitivity at the Rosa26 locus (Fig. 6F), which exhibits lower baseline expression in basal VSNs (Lin et al., 2022) and likely contributes to weaker lineage-tracing signals in this population (Fig. 6F).

In vivo validation confirmed that GfyCre recombination lags behind early differentiation markers such as Gap43, yet robustly labels neurons as they progress toward maturity and project appropriately to both anterior and posterior domains of the accessory olfactory bulb. Together, these findings establish Gfy as a developmentally timed marker of postmitotic vomeronasal neurons, refine the interpretation of Cre-based lineage tracing across VSN subtypes, and provide a framework for selectively manipulating chemosensory neurons without perturbing earlier neurogenic events.

Methods

Animals

Gfy(123)-Cre mice were provided generously from Dr. Thomas Bozza (Northwestern University), originally generated at RIKEN Brain Science Institute, Japan (Dr. Yoshihiro Yoshihara). PCR analysis was performed for genotyping, using generic Cre primers as follows: Cre FWD, AGG TGT AGA GAA GGC ACT TAG C, *Cre RVS, CTA ATC GCC ATC TTC CAG CAG G*. Ai14 mice were genotyped following the B6.Cg-*Gt(ROSA)26Sor*$^{tm14(CAG-tdTomato)Hze}$/J protocols available on jax.org. Generation of Prokr2Cre$^{+/-}$ mice (Mohsen et al. 2017) and genotyping (Amato Jr. et al. 2024) were previously described. CO_2 euthanasia was performed, then immediate cervical dislocation. Mice of either sex were used for experiments. All animal experiments and procedures were completed in accordance with the guidelines of the Animal Care and Use Committee at the University at Albany, SUNY.

Tissue Preparation

Embryonic Tissue Collection

Embryo collection was carefully performed on time-mated females, where observation of the vaginal plug was estimated to be embryonic day 0.5 (E0.5). Collected embryos were placed into 3.7% formaldehyde/PBS at 4°C for 2 h to fix. Embryos then were submerged in 30% sucrose overnight, then embedded and frozen in O.C.T (Tissue-Tek) before storing at −80°C. The CM3050S Leica cryostat was used to cryosection embedded embryos, tissue

404 sections were collected using Superfrost plus slides (VWR) at 18 μm thickness for
405 immunofluorescent staining.
406
407 **Postnatal Tissue Collection**
408 P30 mice were sedated with Sodium Pentobarbital, then transcardial perfusion was
409 performed with 1X PBS followed by 4% Paraformaldehyde in PBS. Noses were separated
410 from brains, with the noses being post fixed in 4% Paraformaldehyde overnight at 4°C.
411 Brains were post fixed in 1% Paraformaldehyde overnight at 4°C. The following day, brains
412 were cryoprotected with 30% Sucrose in 1X PBS at 4°C overnight and noses were incubated
413 in 500mM EDTA in 1X PBS for decalcification. At end of EDTA incubation noses were
414 cryoprotected in sucrose. Samples were embedded and frozen in O.C.T and stored in -80°C
415 prior to cryosectioning serial sections on Superfrost plus (VWR) slides. Noses were
416 sectioned in a coronal orientation, while brains were sectioned in the parasagittal
417 orientation.
418
419
420
421 **Immunohistochemistry**
422 The following primary antibodies and dilutions were used for this study: goat-α-RFP
423 (1:1000, Rockland), chicken-α-Peripherin (1:500, Abcam), SW rabbit-α-GnRH-1 (1:6000,
424 Susan Wray, NIH), rabbit-α-Map2 (1:150, Cell Signaling Technology), mouse-α-RFP (1:500,
425 Origene), rabbit-α-Somatostatin (1:100, Abcam), rabbit-α-Gap43 (1:1000, Abcam), goat-α
426 Neuropilin2 (1:4000, R&D Systems), mouse-α-Robo2 (1:50, Santa Cruz), rabbit-α-RFP
427 (1:500, Rockland), goat-α-OMP (1:4000, WAKO), goat-α-AP-2ε (1:500, R&D Systems), and
428 rabbit-α-Meis2 (1:1000, Abcam).
429
430 Antigen retrieval was used for experiments utilizing rabbit-α-Map2, mouse-α-RFP, goat-α
431 Neuropilin2, mouse-α-Robo2, rabbit-α-RFP, goat-α-AP-2ε, and rabbit-α-Meis2, slides were
432 submerged in a citric acid solution, gradually heated to 95°C, once at 95°C, boiling for

433 15 min. Slides were then cooled for 15 min before proceeding with standard
434 immunohistochemical protocol.
435
436 **Immunofluorescence**
437 For immunofluorescent staining, secondary antibodies selected for the correct species
438 were conjugated with Alexa Fluor-488, Alexa Flour-594, or Alexa Flour-680 (Invitrogen and
439 Jackson Laboratories). 4',6'-diamidino-2-phenylindole (DAPI, 1:3000; Sigma-Aldrich) was
440 used to counterstain sections and coverslips were mounted using Fluorogel l (Electron
441 Microscopy Sciences). Confocal microscopy image acquisition was taken on a LSM 710
442 microscope (Zeiss). Epifluorescence images were acquired on a DM4000 B LED
443 fluorescence microscope equipped with a Leica DFC310 FX camera. Whole embryo
444 images were acquired using the Nikon SMZ25 stereo microscope. Image analysis and
445 quantifications were done using FIJI/ImageJ software. Each staining presented was
446 replicated on three different animals.
447
448 **Edu Administration and Detection**
449 Edu was prepared according to ClickTech EdU Cell Proliferation Kit 488 for IM (Millipore-sigma,
450 BCK-EDU488). Edu injections were performed on time-mated females previously described in
451 the tissue preparation section of the methods. Intraperitoneal injections were done at various
452 time points at a dosage of 50mg/kg body weight. We observed that development was not affected
453 by the injections. To detect Edu positive cells, we performed immunofluorescence as described in
454 the previous section and followed the standard ClickTech EdU Cell Proliferation Kit 488 protocol.
455 Slides were incubated for 30 minutes at room temperature in the prepared detection solution
456 protected from light. After, we followed standard immunofluorescent protocol.
457
458
459 **Cell Quantifications**
460 Quantifications performed were done in FIJI/ImageJ using the cell counter plugin. All cell
461 number quantifications in the nasal region were done on parasaggital E12.0-P1 tissue. For

462 each quantification reported, cell bodies of neurons were counted. For all quantifications
463 of cell counts, the number of cells per section (~5 sections) was averaged for each animal.
464
465
466 **Embryonic Single-Cell Cell RNA Sequencing**
467 Dimplots and feature plots were generated in R studio using the Seurat R package. The
468 E14.5 single-cell sequencing data can be found on the Gene Expression Omnibus (GEO)
469 database: GEO accession number GSE234871
470 (**https://www.ncbi.nlm.nih.gov/geo/query/acc.cgi?acc=GSE234871**). The data
471 collection process and analysis was previously described (Amato Jr. et al. **2024**).
472 **Post-natal scRNA-seq quality control, clustering and analysis.**
473 Quality Control and Filtering: Postnatal single-cell RNA sequencing datasets (P14, P56, and
474 P10, P21, P60) used for analysis can be found with GEO accession numbers GSE247872,
475 and GSE252365. Data collection and analysis were previously described (Hills et al., 2024;
476 LeFever et al., 2024). Independent ages respective datasets were merged and integrated to
477 get a more full picture of the vomeronasal development. Cell filtering was done
478 downstream to remove genes expressed in ≤3 cells, and ≥200 detectable genes. Quality
479 control was done to clean up the data to only cells expressing between 200 and 9000 with
480 ≤25% of those genes being mitochondrial genes.
481 CellCycle Regression: To avoid noise from cells undergoing active cell cycling, cells were
482 scored for their features aligning with S, and G2/M phase as described in a SeuratV5
483 vignette (Hao et al., 2023). The difference between S.Score and G2M.Score was calculated,
484 and these cells were regressed to include differences between cell types but remove
485 differences within cycling cells.
486 DoubletFinder: The DoubletFinder program built for Seurat was applied to reduce and
487 remove a predicted number of artificial doublets created during the process of single cell
488 sequencing. This package was used as previously described (McGinnis et al., 2019).
489 Processing: Using SCTransform the data was scaled and normalized, the top 2000 highly
490 variable features within the top 50 principal components were used for clustering. About

18,000 cells were used in this analysis and different developmental stages were identified through well documented key markers. When completing analysis each cluster/gene were compared against all other clusters/genes. In the Apical/V1R v Basal/V2R comparisons, only the Apical/V1R lineage was compared to the Basal/V2R lineage. Analysis of the differential Gt(ROSA)26Sor expression was conducted on P10, P21, P60 data previously published (LeFever et al., 2024).

Acknowledgements

This work was supported by the Eunice Kennedy Shriver National Institute of Child Health and Human Development (NICHD) under Grants R01HD09733 (P.E.F.) and R01HD114827 (P.E.F.), as well as by the National Institute on Deafness and Other Communication Disorders (NIDCD) under Grant R01DC017149 (P.E.F.). The Zeiss 980 microscope at the University at Albany was funded by the Office of the Director, NIH, under Award Number S10OD028600. We thank Enrico Amato for helping us process the single-cell data and upload it to GEO. We thank Carlsy Ybanez for assisting with Carl4 in-situ hybridization. We thank Nick Mathias for his help with single-cell data processing.

References

Abitua, P. B., Gainous, T. B., Kaczmarczyk, A. N., Winchell, C. J., Hudson, C., Kamata, K., Nakagawa, M., Tsuda, M., Kusakabe, T. G. and Levine, M. (2015). The pre-vertebrate origins of neurogenic placodes. *Nature* **524**, 462-465.

Amato, E., Jr., Semon, A. M. and Forni, P. E. (2025). Tracing Early Migratory Neurons in the Developing Nose Using Contactin-2 (Cntn2) CreERT2. *Genesis* **63**, e70021.

Amato, E., Jr., Taroc, E. Z. M. and Forni, P. E. (2024). Illuminating the terminal nerve: Uncovering the link between GnRH-1 neuron and olfactory development. *J Comp Neurol* **532**, e25599.

Baker, H. and Farbman, A. I. (1993). Olfactory afferent regulation of the dopamine phenotype in the fetal rat olfactory system. *Neuroscience* **52**, 115-134.

Brunjes, P. C. and Frazier, L. L. (1986). Maturation and plasticity in the olfactory system of vertebrates. *Brain research* **396**, 1-45.

Chen, B., Kim, E. H. and Xu, P. X. (2009). Initiation of olfactory placode development and neurogenesis is blocked in mice lacking both Six1 and Six4. *Dev Biol* **326**, 75-85.

526 **Couly, G. F. and Le Douarin, N. M.** (1985). Mapping of the early neural primordium in quail-
527 chick chimeras. I. Developmental relationships between placodes, facial ectoderm, and
528 prosencephalon. *Dev Biol* **110**, 422-439.
529 **Cuschieri, A. and Bannister, L. H.** (1975a). The development of the olfactory mucosa in the
530 mouse: electron microscopy. *Journal of anatomy* **119**, 471-498.
531 **----** (1975b). The development of the olfactory mucosa in the mouse: light microscopy. *Journal of*
532 *anatomy* **119**, 277-286.
533 **Decoster, L., Trova, S., Zucca, S., Bulk, J., Gouveia, A., Ternier, G., Lhomme, T., Legrand,**
534 **A., Gallet, S., Boehm, U., et al.** (2024). A GnRH neuronal population in the olfactory
535 bulb translates socially relevant odors into reproductive behavior in male mice. *Nature*
536 *neuroscience* **27**, 1758-1773.
537 **Demski, L. S. and Schwanzel-Fukuda, M.** (1987). The terminal nerve (nervus terminalis):
538 structure, function, and evolution. Introduction. *Annals of the New York Academy of*
539 *Sciences* **519**, ix-xi.
540 **Enomoto, T., Ohmoto, M., Iwata, T., Uno, A., Saitou, M., Yamaguchi, T., Kominami, R.,**
541 **Matsumoto, I. and Hirota, J.** (2011). Bcl11b/Ctip2 controls the differentiation of
542 vomeronasal sensory neurons in mice. *The Journal of neuroscience : the official journal*
543 *of the Society for Neuroscience* **31**, 10159-10173.
544 **Fornaro, M., Geuna, S., Fasolo, A. and Giacobini-Robecchi, M. G.** (2003). HuC/D confocal
545 imaging points to olfactory migratory cells as the first cell population that expresses a
546 post-mitotic neuronal phenotype in the chick embryo. *Neuroscience* **122**, 123-128.
547 **Forni, P. E., Bharti, K., Flannery, E. M., Shimogori, T. and Wray, S.** (2013). The indirect role
548 of fibroblast growth factor-8 in defining neurogenic niches of the olfactory/GnRH
549 systems. *The Journal of neuroscience : the official journal of the Society for*
550 *Neuroscience* **33**, 19620-19634.
551 **Forni, P. E., Fornaro, M., Guenette, S. and Wray, S.** (2011a). A role for FE65 in controlling
552 GnRH-1 neurogenesis. *The Journal of neuroscience : the official journal of the Society*
553 *for Neuroscience* **31**, 480-491.
554 **Forni, P. E., Taylor-Burds, C., Melvin, V. S., Williams, T. and Wray, S.** (2011b). Neural crest
555 and ectodermal cells intermix in the nasal placode to give rise to GnRH-1 neurons,
556 sensory neurons, and olfactory ensheathing cells. *The Journal of neuroscience : the*
557 *official journal of the Society for Neuroscience* **31**, 6915-6927.
558 **Forni, P. E. and Wray, S.** (2015). GnRH, anosmia and hypogonadotropic hypogonadism--where
559 are we? *Frontiers in neuroendocrinology* **36**, 165-177.
560 **Gong, Q. and Shipley, M. T.** (1995). Evidence that pioneer olfactory axons regulate
561 telencephalon cell cycle kinetics to induce the formation of the olfactory bulb. *Neuron* **14**,
562 91-101.
563 **Graham, A., Blentic, A., Duque, S. and Begbie, J.** (2007). Delamination of cells from
564 neurogenic placodes does not involve an epithelial-to-mesenchymal transition.
565 *Development* **134**, 4141-4145.
566 **Guillemot, F., Lo, L. C., Johnson, J. E., Auerbach, A., Anderson, D. J. and Joyner, A. L.**
567 (1993). Mammalian achaete-scute homolog 1 is required for the early development of
568 olfactory and autonomic neurons. *Cell* **75**, 463-476.
569 **Habif, J. C., Xie, C., de Celis, C., Ukhanov, K., Green, W. W., Moretta, J. C., Zhang, L.,**
570 **Campbell, R. J. and Martens, J. R.** (2023). The role of a ciliary GTPase in the
571 regulation of neuronal maturation of olfactory sensory neurons. *Development* **150**.
572 **Hanchate, N. K., Giacobini, P., Lhuillier, P., Parkash, J., Espy, C., Fouveaut, C., Leroy, C.,**
573 **Baron, S., Campagne, C., Vanacker, C., et al.** (2012). SEMA3A, a gene involved in
574 axonal pathfinding, is mutated in patients with Kallmann syndrome. *PLoS genetics* **8**,
575 e1002896.

Herbison, A. E. (2025). Evolution of the GnRH Neuron. In *Evolutionary and Comparative Neuroendocrinology* (ed. V. Grinevich & R. Oliveira), pp. 143-164. Cham: Springer Nature Switzerland.

Hilal, E. M., Chen, J. H. and Silverman, A. J. (1996). Joint migration of gonadotropin-releasing hormone (GnRH) and neuropeptide Y (NPY) neurons from olfactory placode to central nervous system. *Journal of neurobiology* **31**, 487-502.

Hills, M. H., Ma, L., Fang, A., Chiremba, T., Malloy, S., Scott, A. R., Perera, A. G. and Yu, C. R. (2024). Molecular, cellular, and developmental organization of the mouse vomeronasal organ at single cell resolution. *eLife* **13**.

Hirata, T., Nakazawa, M., Yoshihara, S., Miyachi, H., Kitamura, K., Yoshihara, Y. and Hibi, M. (2006). Zinc-finger gene Fez in the olfactory sensory neurons regulates development of the olfactory bulb non-cell-autonomously. *Development* **133**, 1433-1443.

Ikeda, K., Ookawara, S., Sato, S., Ando, Z., Kageyama, R. and Kawakami, K. (2007). Six1 is essential for early neurogenesis in the development of olfactory epithelium. *Dev Biol* **311**, 53-68.

Jasoni, C. L., Porteous, R. W. and Herbison, A. E. (2009). Anatomical location of mature GnRH neurons corresponds with their birthdate in the developing mouse. *Developmental dynamics : an official publication of the American Association of Anatomists* **238**, 524-531.

Kallmann, F. (1944). The genetic aspects of primary eunuchoidism.

Kamiya, C., Ohta, N., Ogura, Y., Yoshida, K., Horie, T., Kusakabe, T. G., Satake, H. and Sasakura, Y. (2014). Nonreproductive role of gonadotropin-releasing hormone in the control of ascidian metamorphosis. *Developmental dynamics : an official publication of the American Association of Anatomists* **243**, 1524-1535.

Kaneko-Goto, T., Sato, Y., Katada, S., Kinameri, E., Yoshihara, S., Nishiyori, A., Kimura, M., Fujita, H., Touhara, K., Reed, R. R., et al. (2013). Goofy coordinates the acuity of olfactory signaling. *The Journal of neuroscience : the official journal of the Society for Neuroscience* **33**, 12987-12996, 12996a.

Karns, L. R., Ng, S. C., Freeman, J. A. and Fishman, M. C. (1987). Cloning of complementary DNA for GAP-43, a neuronal growth-related protein. *Science* **236**, 597-600.

Katoh, H., Shibata, S., Fukuda, K., Sato, M., Satoh, E., Nagoshi, N., Minematsu, T., Matsuzaki, Y., Akazawa, C., Toyama, Y., et al. (2011). The dual origin of the peripheral olfactory system: placode and neural crest. *Molecular brain* **4**, 34.

Katreddi, R. R., Taroc, E. Z. M., Hicks, S. M., Lin, J. M., Liu, S. T., Xiang, M. Q. and Forni, P. E. (2022). Notch signaling determines cell-fate specification of the two main types of vomeronasal neurons of rodents. *Development* **149**.

Klein, S. L. and Graziadei, P. P. (1983). The differentiation of the olfactory placode in Xenopus laevis: a light and electron microscope study. *J Comp Neurol* **217**, 17-30.

LeFever, N. M., Katreddi, R. R., Dolphin, N. M., Mathias, N. A. and Forni, P. E. (2024). Following the p63/Keratin5 basal cells in the sensory and non-sensory epithelia of the vomeronasal organ. *Genesis* **62**, e23596.

Lieblich, J. M., Rogol, A. D., White, B. J. and Rosen, S. W. (1982). Syndrome of anosmia with hypogonadotropic hypogonadism (Kallmann syndrome): clinical and laboratory studies in 23 cases. *The American journal of medicine* **73**, 506-519.

Lin, J. M., Mitchell, T. A., Rothstein, M., Pehl, A., Taroc, E. Z. M., Katreddi, R. R., Parra, K. E., Zuloaga, D. G., Simoes-Costa, M. and Forni, P. E. (2022). Sociosexual behavior requires both activating and repressive roles of Tfap2e/AP-2epsilon in vomeronasal sensory neurons. *eLife* **11**.

Lin, J. M., Taroc, E. Z. M., Frias, J. A., Prasad, A., Catizone, A. N., Sammons, M. A. and Forni, P. E. (2018). The transcription factor Tfap2e/AP-2epsilon plays a pivotal role in maintaining the identity of basal vomeronasal sensory neurons. *Dev Biol* **441**, 67-82.

Lund, C., Yellapragada, V., Vuoristo, S., Balboa, D., Trova, S., Allet, C., Eskici, N., Pulli, K., Giacobini, P., Tuuri, T., et al. (2020). Characterization of the human GnRH neuron developmental transcriptome using a GNRH1-TdTomato reporter line in human pluripotent stem cells. *Dis Model Mech* **13**.

Margolis, F. L. (1972). A brain protein unique to the olfactory bulb. *Proc Natl Acad Sci U S A* **69**, 1221-1224.

Margolis, F. L. and Tarnoff, J. F. (1973). Site of biosynthesis of the mouse brain olfactory bulb protein. *The Journal of biological chemistry* **248**, 451-455.

Miller, A. M., Treloar, H. B. and Greer, C. A. (2010). Composition of the migratory mass during development of the olfactory nerve. *J Comp Neurol* **518**, 4825-4841.

Murakami, S., Ohki-Hamazaki, H. and Uchiyama, Y. (2022). Olfactory placode generates a diverse population of neurons expressing GnRH, somatostatin mRNA, neuropeptide Y, or calbindin in the chick forebrain. *J Comp Neurol* **530**, 2977-2993.

---- (2024). Somatostatin affects GnRH neuronal development and migration and stimulates olfactory-related fiber fasciculation. *Developmental neurobiology* **84**, 3-17.

Paronett, E. M., Bryan, C. A., Maynard, T. M. and LaMantia, A.-S. (2023). Identity, lineage and fates of a temporally distinct progenitor population in the embryonic olfactory epithelium. *Developmental biology*.

Poncelet, G. and Shimeld, S. M. (2020). The evolutionary origins of the vertebrate olfactory system. *Open Biol* **10**, 200330.

Rawson, N. E. (1999). Cell and molecular biology of olfaction. *Quintessence Int* **30**, 335-341.

Rawson, N. E., Lischka, F. W., Yee, K. K., Peters, A. Z., Tucker, E. S., Meechan, D. W., Zirlinger, M., Maynard, T. M., Burd, G. B., Dulac, C., et al. (2010). Specific mesenchymal/epithelial induction of olfactory receptor, vomeronasal, and gonadotropin-releasing hormone (GnRH) neurons. *Developmental dynamics : an official publication of the American Association of Anatomists* **239**, 1723-1738.

Rukh, S., Meechan, D. W., Maynard, T. M. and Lamantia, A. S. (2024). Out of Line or Altered States? Neural Progenitors as a Target in a Polygenic Neurodevelopmental Disorder. *Dev Neurosci* **46**, 1-21.

Sakai, T., Yamamoto, T., Matsubara, S., Kawada, T. and Satake, H. (2020). Invertebrate Gonadotropin-Releasing Hormone Receptor Signaling and Its Relevant Biological Actions. *Int J Mol Sci* **21**.

Schwanzel-Fukuda, M. and Pfaff, D. W. (1989). Origin of luteinizing hormone-releasing hormone neurons. *Nature* **338**, 161-164.

Schwarting, G. A., Kostek, C., Bless, E. P., Ahmad, N. and Tobet, S. A. (2001). Deleted in colorectal cancer (DCC) regulates the migration of luteinizing hormone-releasing hormone neurons to the basal forebrain. *The Journal of neuroscience : the official journal of the Society for Neuroscience* **21**, 911-919.

Shan, Y., Saadi, H. and Wray, S. (2020). Heterogeneous Origin of Gonadotropin Releasing Hormone-1 Neurons in Mouse Embryos Detected by Islet-1/2 Expression. *Front Cell Dev Biol* **8**, 35.

Smart, I. H. (1971). Location and orientation of mitotic figures in the developing mouse olfactory epithelium. *Journal of anatomy* **109**, 243-251.

Stolfi, A., Ryan, K., Meinertzhagen, I. A. and Christiaen, L. (2015). Migratory neuronal progenitors arise from the neural plate borders in tunicates. *Nature* **527**, 371-374.

Taroc, E. Z. M., Lin, J. M., Tulloch, A. J., Jaworski, A. and Forni, P. E. (2019). GnRH-1 Neural Migration From the Nose to the Brain Is Independent From Slit2, Robo3 and NELL2 Signaling. *Front Cell Neurosci* **13**, 70.

Taroc, E. Z. M., Naik, A. S., Lin, J. M., Peterson, N. B., Keefe, D. L., Jr., Genis, E., Fuchs, G., Balasubramanian, R. and Forni, P. E. (2020). Gli3 Regulates Vomeronasal Neurogenesis, Olfactory Ensheathing Cell Formation, and GnRH-1 Neuronal Migration.

The Journal of neuroscience : the official journal of the Society for Neuroscience **40**, 311-326.

Taroc, E. Z. M., Prasad, A., Lin, J. M. and Forni, P. E. (2017). The terminal nerve plays a prominent role in GnRH-1 neuronal migration independent from proper olfactory and vomeronasal connections to the olfactory bulbs. *Biol Open* **6**, 1552-1568.

Tarozzo, G., Peretto, P. and Fasolo, A. (1995). Cell migration from the olfactory placode and the ontogeny of the neuroendocrine compartments. *Zoolog Sci* **12**, 367-383.

Umatani, C. and Oka, Y. (2019). Multiple functions of non-hypophysiotropic gonadotropin releasing hormone neurons in vertebrates. *Zoological Lett* **5**, 23.

Valverde, F., Heredia, M. and Santacana, M. (1993). Characterization of neuronal cell varieties migrating from the olfactory epithelium during prenatal development in the rat. Immunocytochemical study using antibodies against olfactory marker protein (OMP) and luteinizing hormone-releasing hormone (LH-RH). *Brain research. Developmental brain research* **71**, 209-220.

Verhaagen, J., Oestreicher, A. B., Gispen, W. H. and Margolis, F. L. (1989). The expression of the growth associated protein B50/GAP43 in the olfactory system of neonatal and adult rats. *The Journal of neuroscience : the official journal of the Society for Neuroscience* **9**, 683-691.

Verwoerd, C. D. and van Oostrom, C. G. (1979). Cephalic neural crest and placodes. *Adv Anat Embryol Cell Biol* **58**, 1-75.

Vilensky, J. A. (2012). The neglected cranial nerve: Nervus terminalis (cranial nerve N). *Clin Anat*.

Whitlock, K. E. and Westerfield, M. (2000). The olfactory placodes of the zebrafish form by convergence of cellular fields at the edge of the neural plate. *Development* **127**, 3645-3653.

Wierman, M. E., Kiseljak-Vassiliades, K. and Tobet, S. (2011). Gonadotropin-releasing hormone (GnRH) neuron migration: initiation, maintenance and cessation as critical steps to ensure normal reproductive function. *Frontiers in neuroendocrinology* **32**, 43-52.

Wray, S., Grant, P. and Gainer, H. (1989). Evidence that cells expressing luteinizing hormone-releasing hormone mRNA in the mouse are derived from progenitor cells in the olfactory placode. *Proceedings of the National Academy of Sciences of the United States of America* **86**, 8132-8136.

Yoshida, K., Tobet, S. A., Crandall, J. E., Jimenez, T. P. and Schwarting, G. A. (1995). The migration of luteinizing hormone-releasing hormone neurons in the developing rat is associated with a transient, caudal projection of the vomeronasal nerve. *The Journal of neuroscience : the official journal of the Society for Neuroscience* **15**, 7769-7777.

Zouaghi, Y., Alpern, D., Gardeux, V., Russeil, J., Deplancke, B., Santoni, F., Pitteloud, N. and Messina, A. (2025). Transcriptomic profiling of murine GnRH neurons reveals developmental trajectories linked to human reproduction and infertility. *Theranostics* **15**, 3673-3692.

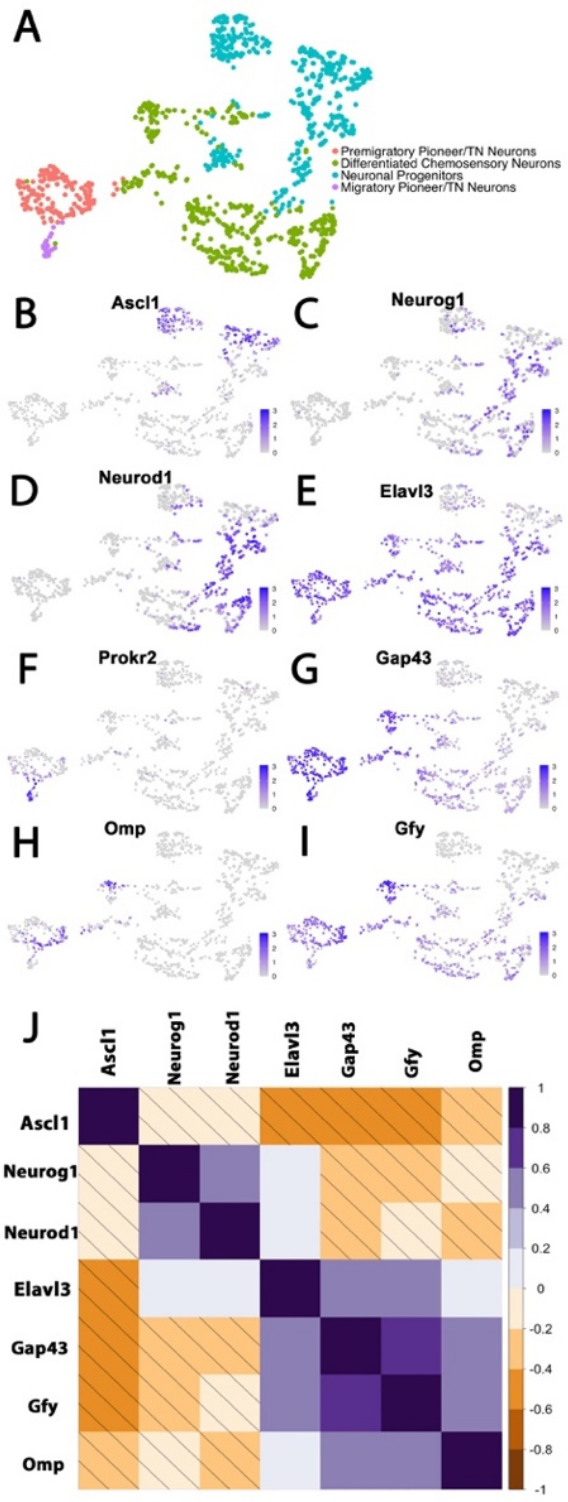
A
Premigratory Pioneer/TN Neurons
Differentiated Chemosensory Neurons
Neuronal Progenitors
Migratory Pioneer/TN Neurons
B
Ascl1
C
Neurog1
D
Neurod1
E
Elavl3
F
Prokr2
G
Gap43
H
Omp
I
Gfy
J
Ascl1
Neurog1
Neurod1
Elavl3
Gap43
Gfy
Omp
1
0.8
0.6
0.4
0.2
0
-0.2
-0.4
-0.6
-0.8
-1

Figure 1. Gfy expression in the developing olfactory system.
A) UMAP of neuronal populations in the developing olfactory system at E14.5 generated from single-cell RNA sequencing of the nasal area. B–I) Feature plots showing expression of for Ascl1, Neurog1, Neurod1, Elav3, Prokr2, Gap43, Omp, and Gfy. Progenitor markers (Ascl1, Neurog1) precede neuronal differentiation markers (Neurod1, Elavl3), while Gap43 labels immature neurons and Omp marks mature sensory neurons. Gfy is enriched in differentiating and immature neuronal populations. J) Correlation matrix showing negative correlations (diagonal lines) between progenitor and maturation markers and positive correlations between Gfy and neuronal differentiation genes.

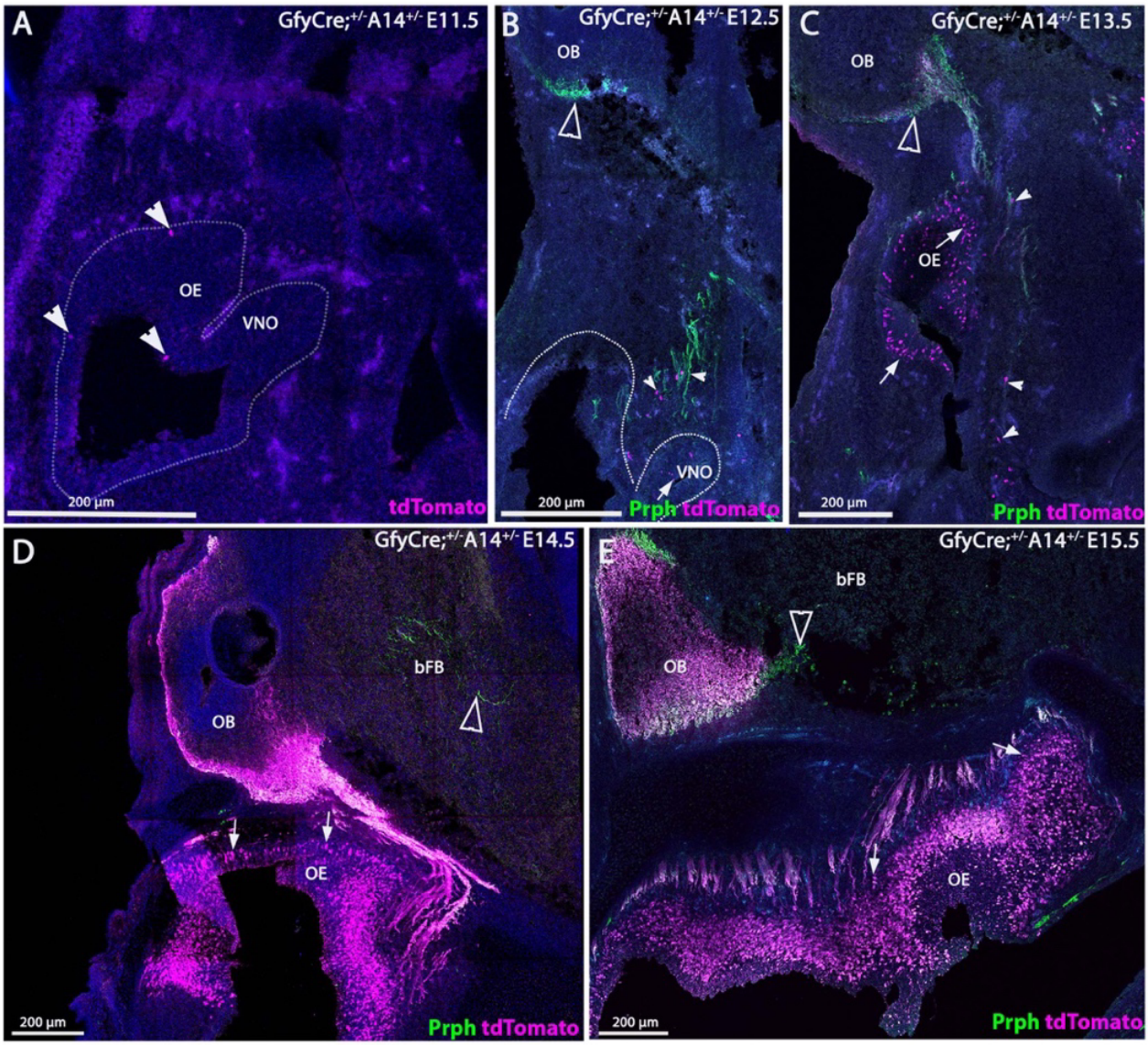

Figure 2. Time course of Gfy genetic lineage tracing in the developing olfactory system. A) At E11.5, GfyCre$^{+/-}$;Ai14$^{+/-}$ parasagittal sections show sparse Gfy lineage tracing (magenta) in the olfactory epithelium (OE) and vomeronasal organ (VNO). B) At E12.5, Gfy tracing is detected in both chemosensory neurons (tailed arrows) and migratory neurons (white notched arrowheads), closely associated with peripherin-positive fibers (Prph, green), including near the olfactory bulb (OB). C) At E13.5, Gfy-traced cells are present in the OE (tailed arrows) and within the peripherin-positive migratory mass (notched arrowheads); peripherin-positive axons positive for the tracing are visible near the OB (open arrowhead).

D–E) At E14.5 and E15.5, Gfy tracing becomes abundant throughout the nasal epithelium, particularly in the OE (tailed arrows). In contrast, Peripherin-positive axons projecting to the basal forebrain and peripherin positive migratory neurons in the basal forebrain (bFB) are largely Gfy-negative (open arrowheads). Scale bars, 200 µm.

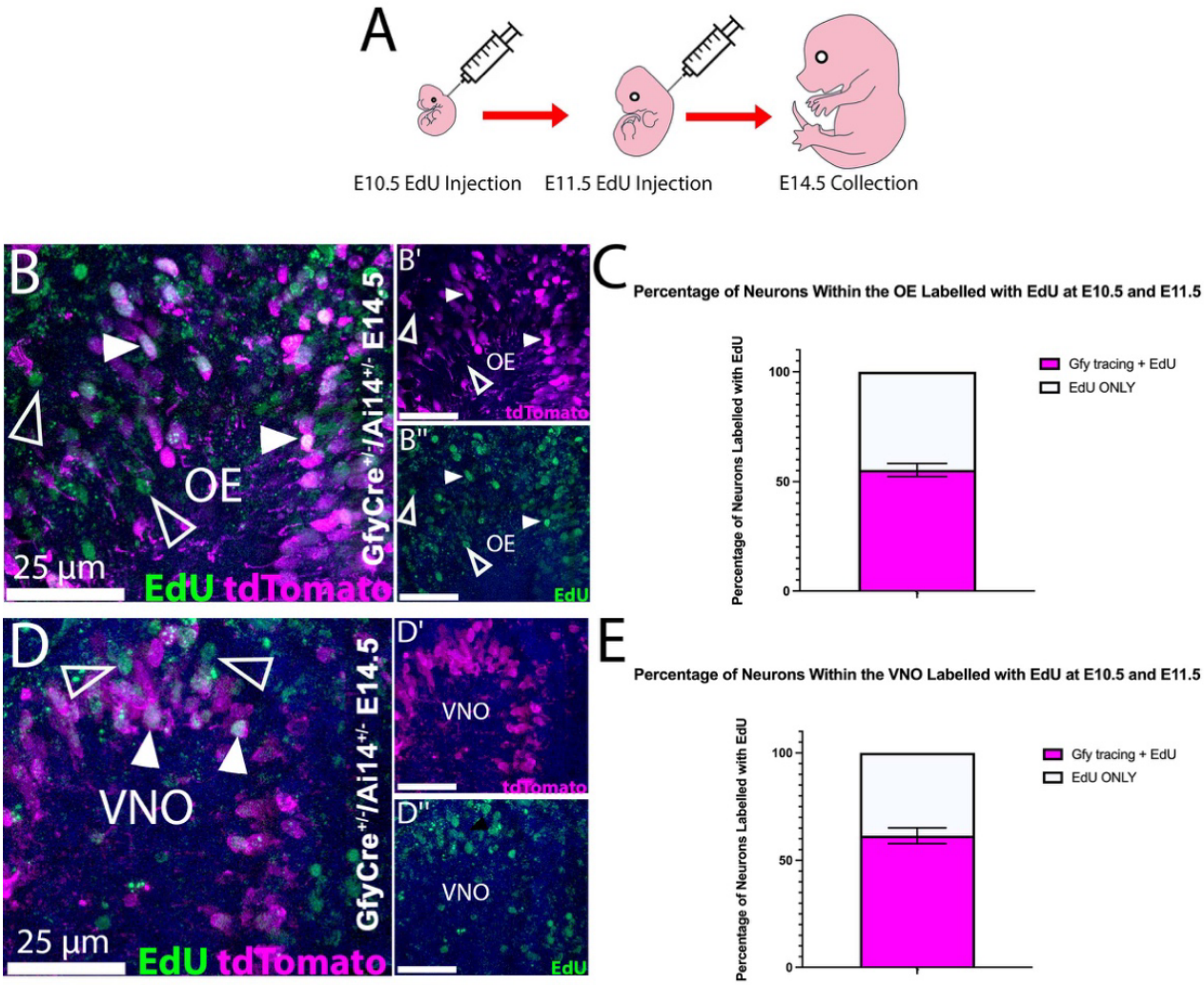

Figure 3. Gfy lineage tracing labels early-born chemosensory neurons.
A) Schematic of EdU birth-dating experiments: EdU injections at E10.5 and E11.5 followed by tissue collection at E14.5. B–B") GfyCre+/−;Ai14+/− E14.5 olfactory epithelium (OE) sections stained for EdU (green) and Gfy lineage tracing (tdTomato, magenta). Gfy-traced neurons (open arrowheads) include a substantial fraction that is EdU-positive (filled arrowheads). C) Quantification of EdU-positive neurons in the OE showing the proportion that is Gfy-traced versus EdU-only. D–D") GfyCre+/−;Ai14+/− E14.5 vomeronasal organ (VNO) sections stained for EdU and Gfy tracing. E) Quantification of EdU-positive neurons in the VNO showing the proportion that is Gfy-traced versus EdU-only. Scale bars, 25 µm.

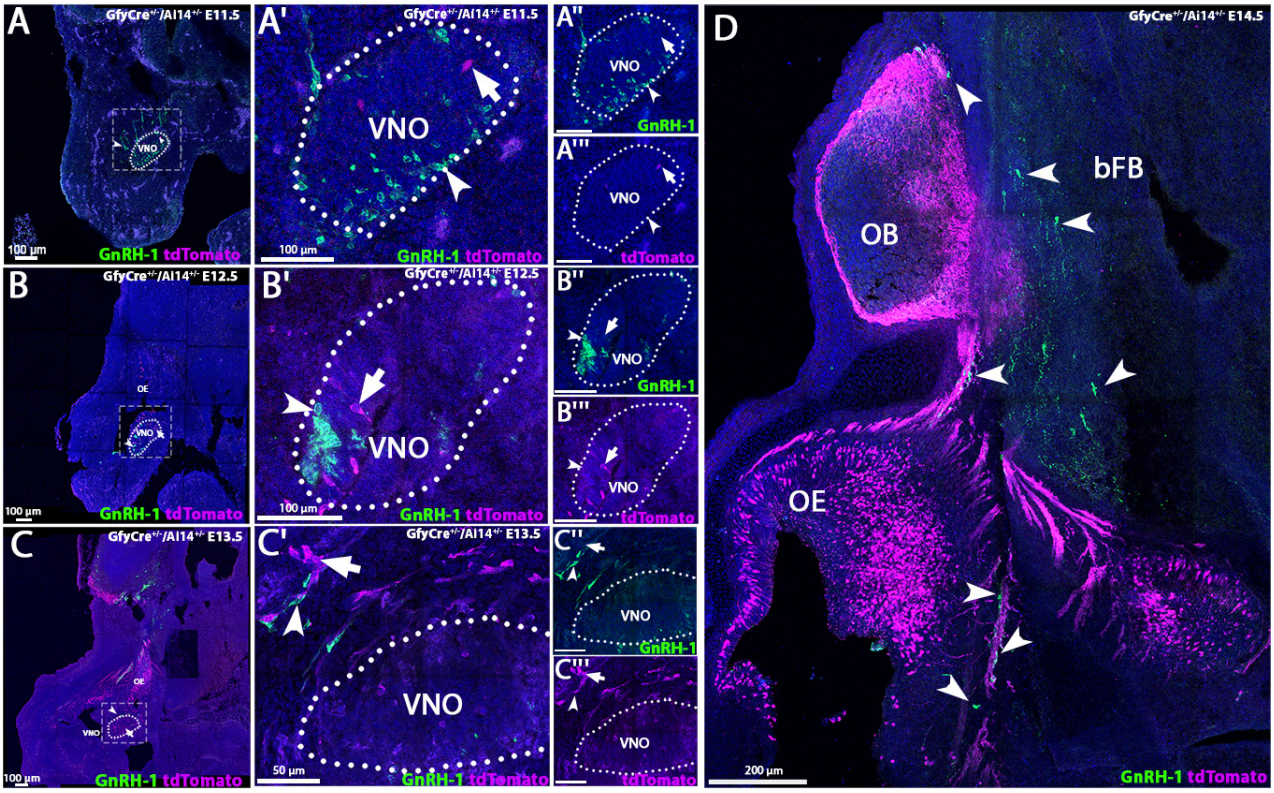

Figure 4. GnRH-1 neurons do not express Gfy.
Parasagittal sections from GfyCre$^{+/-}$;Ai14$^{+/-}$ embryos at E11.5-E14.5 stained for GnRH-1 (green)(arrowheads). A-A‴) At E11.5, GnRH-1 neurons are located within and emerging from the vomeronasal organ (VNO), while Gfy lineage tracing (magenta) is sparse (arrows). B-B‴) At E12.5, Gfy-traced neurons increase in the VNO and olfactory epithelium (OE), coinciding with continued GnRH-1 neuronal migration. C-C‴) By E13.5, GnRH-1 neurons begin invading the brain, whereas Gfy tracing remains restricted to the nasal compartment. D) At E14.5, GnRH-1 neurons reach the basal forebrain (bFB); Gfy tracing is abundant in the nasal epithelium and detectable in the olfactory bulb (OB) but remains absent from GnRH-1 neurons. Scale bars: D, 200 µm; A-C and A'-B‴, 100 µm; C'-C‴, 50 µm.

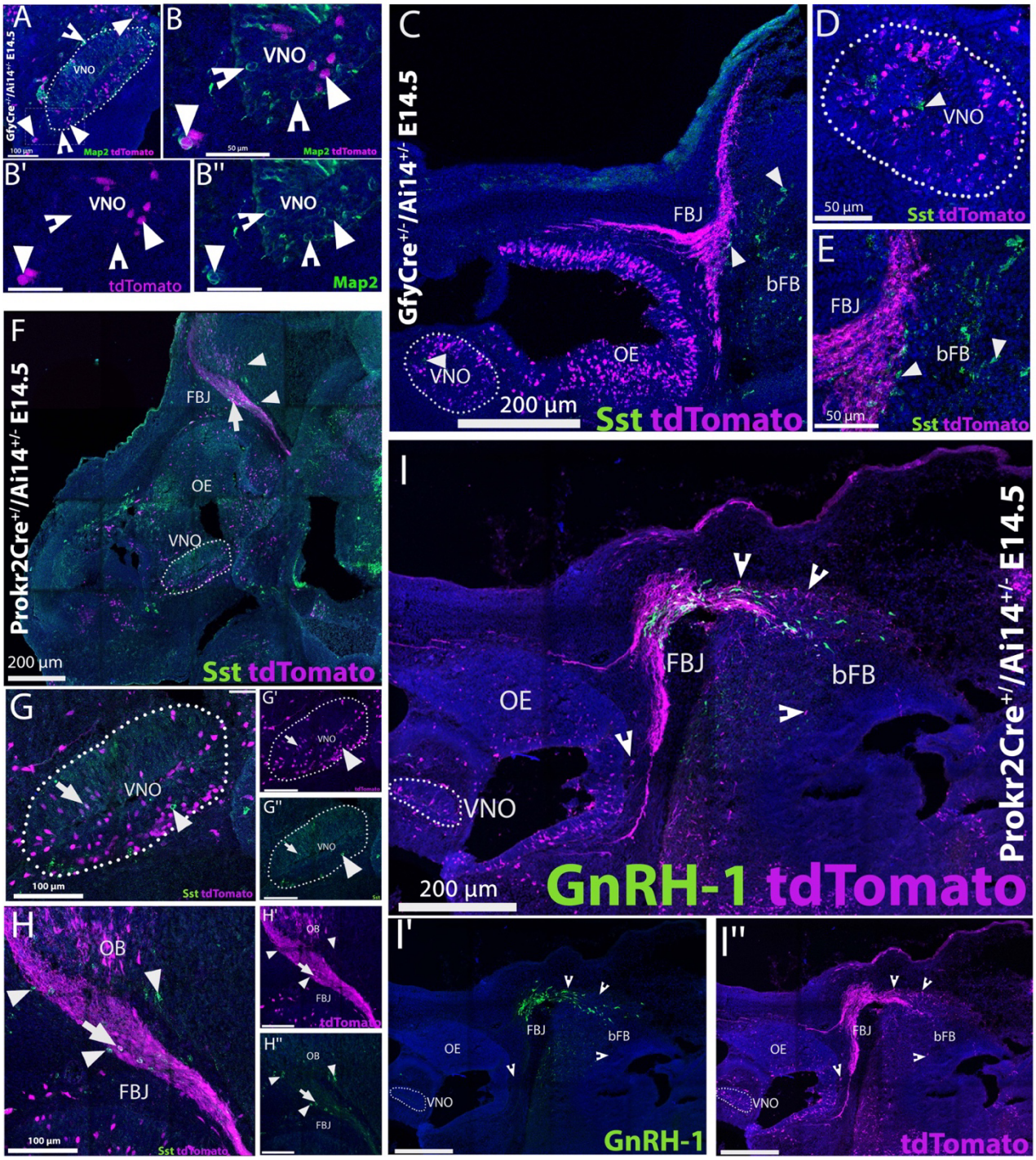

Figure 5. A subpopulation of the migratory mass neurons express Gfy, but do not invade the brain.

A-B'') GfyCre$^{+/-}$/Ai14$^{+/-}$ embryos at E13.5 paired with TN marker Map2 (green) immunofluorescent staining (notched arrows). Many Map2+ TN neurons were observed to migrate in clusters out of the vomeronasal organ (VNO). Gfy traced neurons (magenta)

818 were observed in the VNO, and olfactory epithelium (OE) and migratory mass. Many of the
819 migratory Gfy traced neurons appeared to be Map2+ (arrows). C-E) E14.5 GfyCre$^{+/-}$/Ai14$^{+/-}$
820 embryos stained for Somatostatin (Sst, green). Sst neurons in the migratory mass near the
821 forebrain junction (FBJ) and basal forebrain (bFB) are not positive for Gfy tracing
822 (arrowheads). F-H'') Prokr2Cre$^{+/-}$/Ai14$^{+/-}$ E14.5 sections stained with Sst. Prokr2 tracing
823 appears to overlap with Sst expression in both the VNO and migratory mass near the FBJ. I-
824 I'') Prokr2Cre$^{+/-}$/Ai14$^{+/-}$ E14.5 embryos paired with GnRH-1 immunofluorescent staining.
825 Prokr2 traced cell bodies and fibers migrate from the nose (notched arrowheads) invade
826 the brain, distinct from the GnRH-1 neurons. Scale bars in C,F,I-I'', 200 μm; A, G-G'', H-H'',
827 100 μm; B-B'', D,E, G-G'', 50 μm.

828

829

830

831

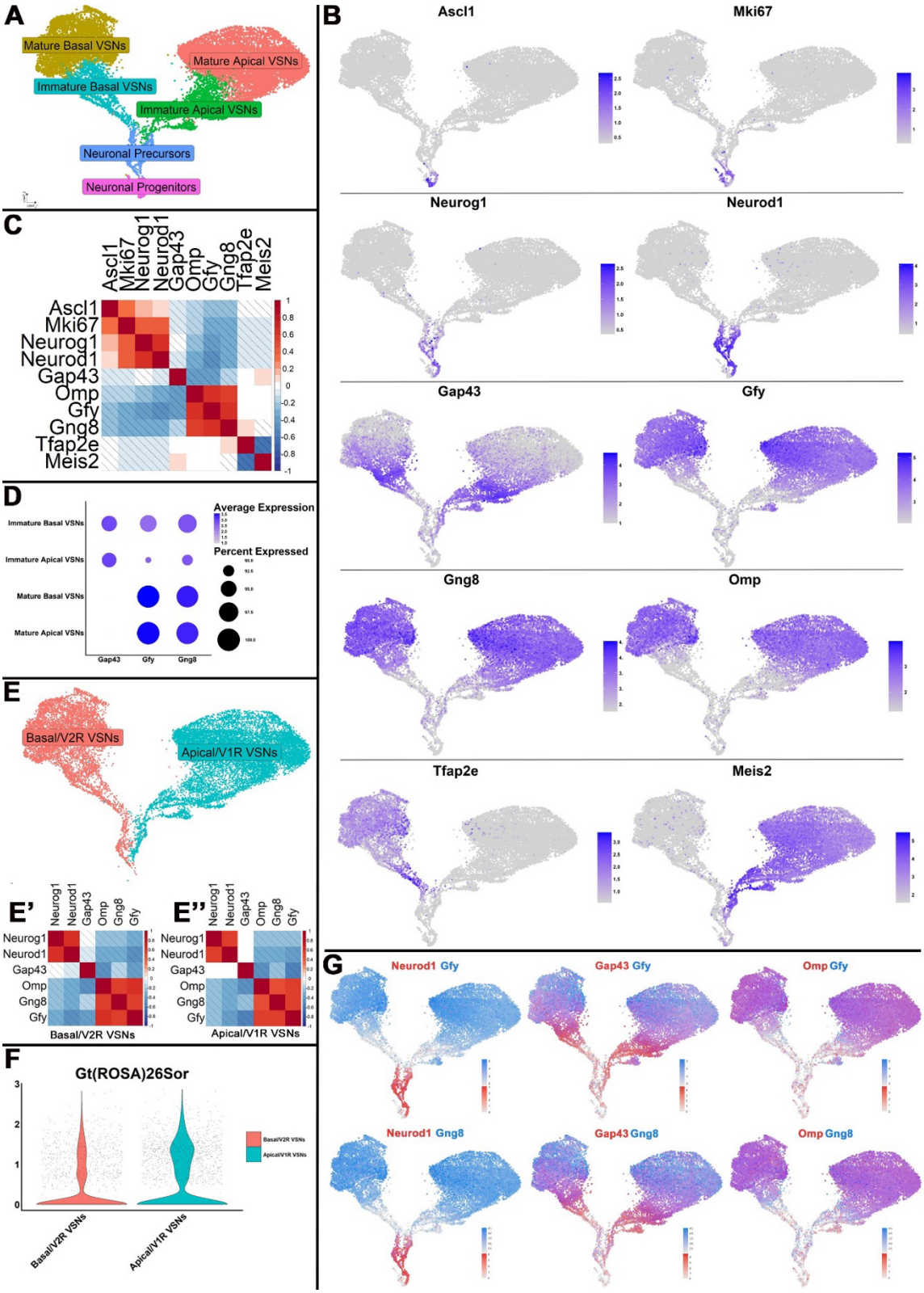
A
Mature Basal VSNs
Mature Apical VSNs
Immature Basal VSNs
Immature Apical VSNs
Neuronal Precursors
Neuronal Progenitors
B
Ascl1
Mki67
Neurog1
Neurod1
Gap43
Gfy
Gng8
Omp
Tfap2e
Meis2
C
Ascl1
Mki67
Neurog1
Neurod1
Gap43
Omp
Gfy
Gng8
Tfap2e
Meis2
D
Immature Basal VSNs
Immature Apical VSNs
Mature Basal VSNs
Mature Apical VSNs
Gap43
Gfy
Gng8
Average Expression
Percent Expressed
E
Basal/V2R VSNs
Apical/V1R VSNs
E'
E''
Neurog1
Neurod1
Gap43
Omp
Gng8
Gfy
Basal/V2R VSNs
Apical/V1R VSNs
F
Gt(ROSA)26Sor
Basal/V2R VSNs
Apical/V1R VSNs
G
Neurod1 Gfy
Gap43 Gfy
Omp Gfy
Neurod1 Gng8
Gap43 Gng8
Omp Gng8

Figure 6. Single-cell transcriptomic analysis of the postnatal vomeronasal organ. A) UMAP projection of scRNA-seq data from the postnatal vomeronasal organ illustrating the major neuronal populations, including Neuronal Progenitors, Neuronal Precursors, Immature apical and basal VSNs, and mature V1R/Meis2+ and V2R/AP-2ε+ VSNs. The characteristic Y-shaped dichotomy of apical and basal lineages is resolved. B) UMAP feature plots showing expression of key developmental markers across the dataset. Ascl1 and Mki67 label proliferative progenitors, Neurog1 and Neurod1 label neuronal precursors, Gap43 marks immature neurons of both lineages, whereas Omp labels mature VSNs. Gfy and Gng8 are associated with early postmitotic neuronal states. Tfap2e and Meis2 highlight the basal and apical lineages, respectively. C) Correlation matrix illustrating co-expression patterns among canonical developmental and lineage-specific markers. Strong positive correlations identify the sequential transitions from progenitors to neuronal precursors to immature and mature VSNs. Negative correlations indicated with diagonal lines. D) Dot plot summarizing Gap43, Gfy, and Gng8 expression across immature and mature apical and basal VSNs. Average expression and percent of expressing cells show that Gfy and Gng8 are lowly expressed in immature stages and are enriched upon maturation. E) UMAP projections showing the apical (V1R/Meis2+) and basal (V2R/Tfap2e+) VSN lineages segregated for comparison. E'–E") Correlation matrices demonstrating that the developmental progression of apical and basal VSNs involves similar transcriptional transitions, but with distinct lineage-specific marker relationships. F) Violin plots comparing expression of the Gt(ROSA)26Sor locus between basal and apical VSNs, revealing differential baseline activity of the ROSA locus across lineages. (G) Co-expression UMAPs illustrating the spatial and developmental relationships of Gfy and Gng8 with Neurod1, Gap43, and Omp, highlighting that Gfy and Gng8 mark neurons before and after they reach full maturation.

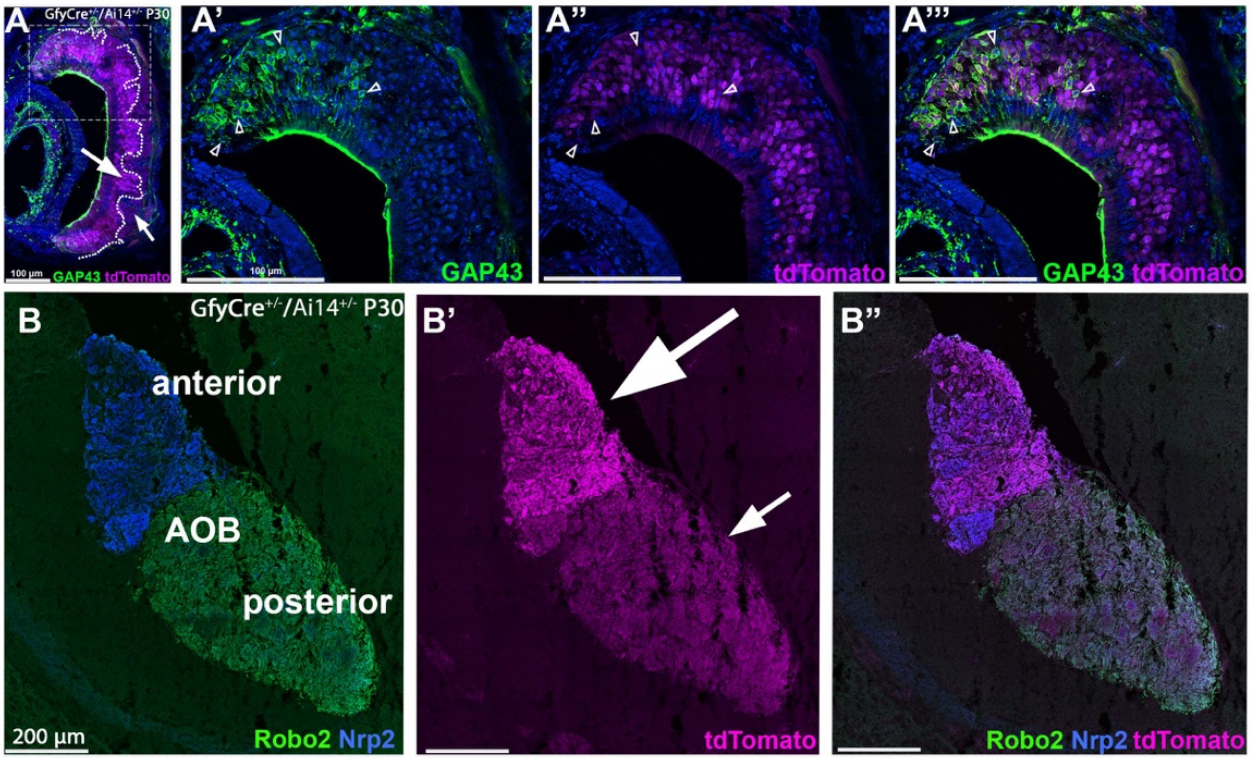

Figure 7. GfyCre-traced neurons in the VNO and AOB exhibit distinct levels of Gfy expression. A) Postnatal day 30 (P30) GfyCre$^{+/-}$;Ai14$^{+/-}$ vomeronasal organ (VNO) coronal sections stained for the immature vomeronasal sensory neuron (VSN) marker Gap43 (green) and tdTomato (red). Gfy lineage tracing (magenta) is detected at lower levels in neurons in the basal territories (small arrows) and at higher levels in VSNs in the apical regions (larger arrows). A'-A''' enlargements of the marginal zone (boxed in (A)) showing GAP43; tdTomato and merge A'''). Arrows indicate GAP43 immunoreactive cells negative for tdTomato or expressing below detectability. B–B") P30 GfyCre$^{+/-}$;Ai14$^{+/-}$ accessory olfactory bulb (AOB) sections stained for Robo2 (green) and Nrp2 (blue) to distinguish posterior and anterior AOB projections, respectively. B'-B") GfyCre tracing (magenta) is present in both anterior and posterior AOB regions but appears weaker in the Nrp2-positive posterior AOB (small arrows) compared with the anterior AOB (large arrows). Scale bars: A–A''', 100 µm; B–B", 200 µm.

Supplementary Figures

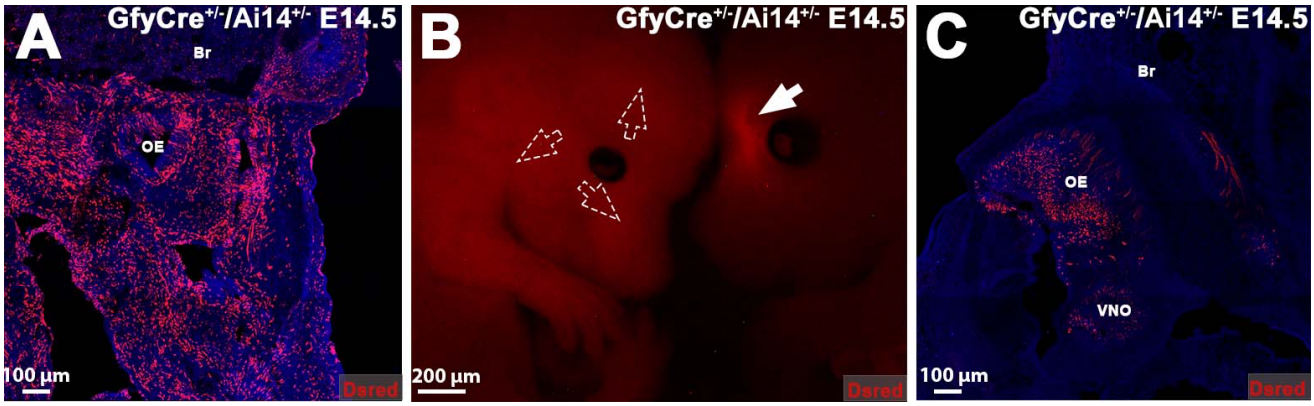

Figure S1.
GfyCre Non-specific Recombination.
A) An E14.5 GfyCre$^{+/-}$/Ai14$^{+/-}$ with nonspecific, broad chimeric tracing throughout the nasal area including the olfactory epithelium (OE). B) Whole-embryo imaging comparing a GfyCre$^{+/-}$/Ai14$^{+/-}$ embryo with nonspecific tracing present throughout the whole body (left) and a GfyCre$^{+/-}$/Ai14$^{+/-}$ embryo with correct tracing exclusive to the olfactory system (right, arrow). C) A correctly traced GfyCre$^{+/-}$/Ai14$^{+/-}$ E14.5 embryo, Gfy tracing can be visualized in the developing vomeronasal organ (VNO) and OE. Scale bars in B, 200 µm; A,C, 100 µm.

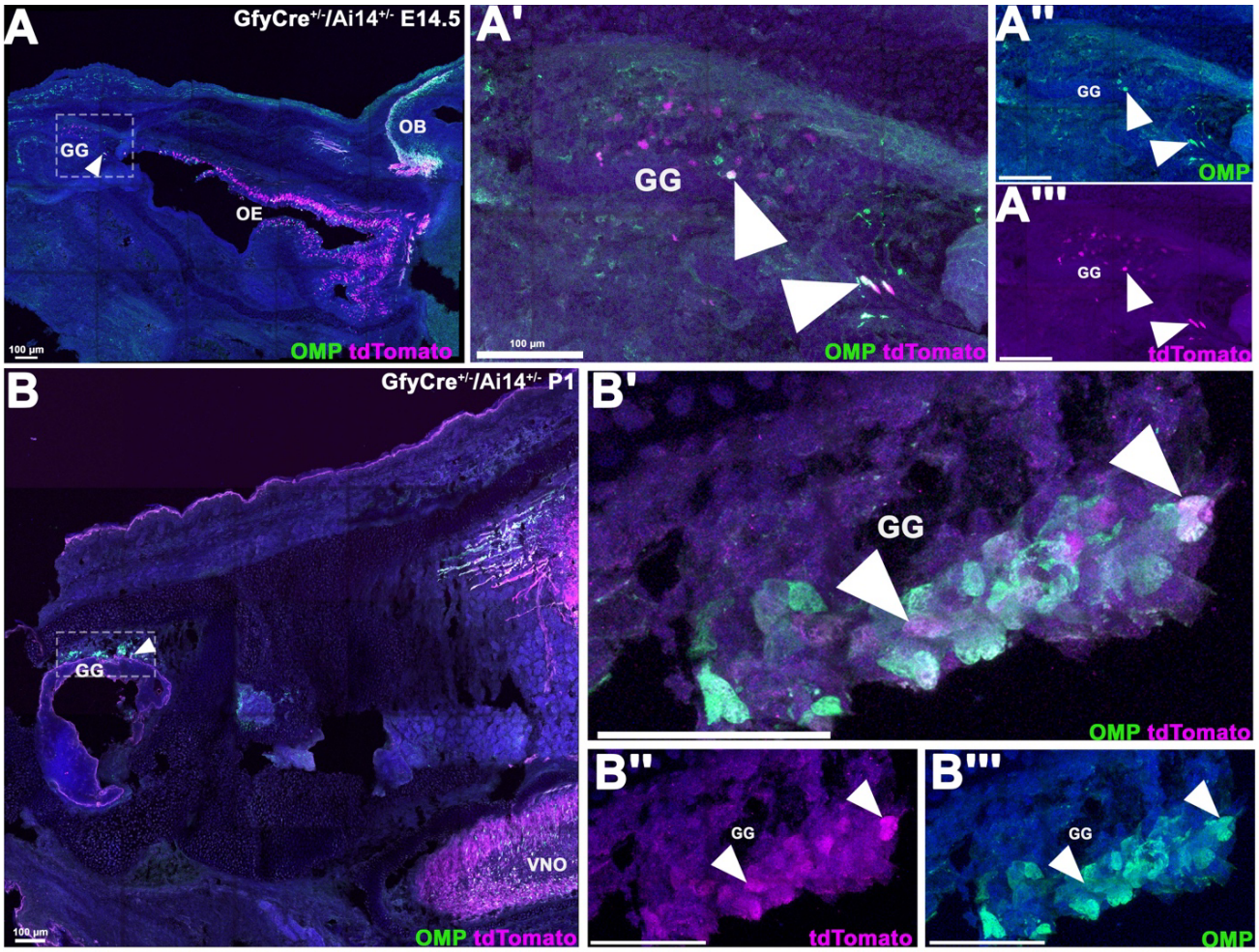

Figure S2.

The Grueneberg Ganglion Expresses Gfy.

A-A''') E14.5 GfyCre$^{+/-}$/Ai14$^{+/-}$ embryos immunostained for Omp (green). Gfy tracing can be observed in the olfactory bulb (OB), olfactory epithelium (OE) and the neurons of the Grueneberg ganglion (GG) (arrowheads). B-B''') P2 GfyCre$^{+/-}$/Ai14$^{+/-}$ animals show increased Gfy tracing in the vomeronasal organ (VNO) and GG. Scale bars in A-B''', D, 100 µm.

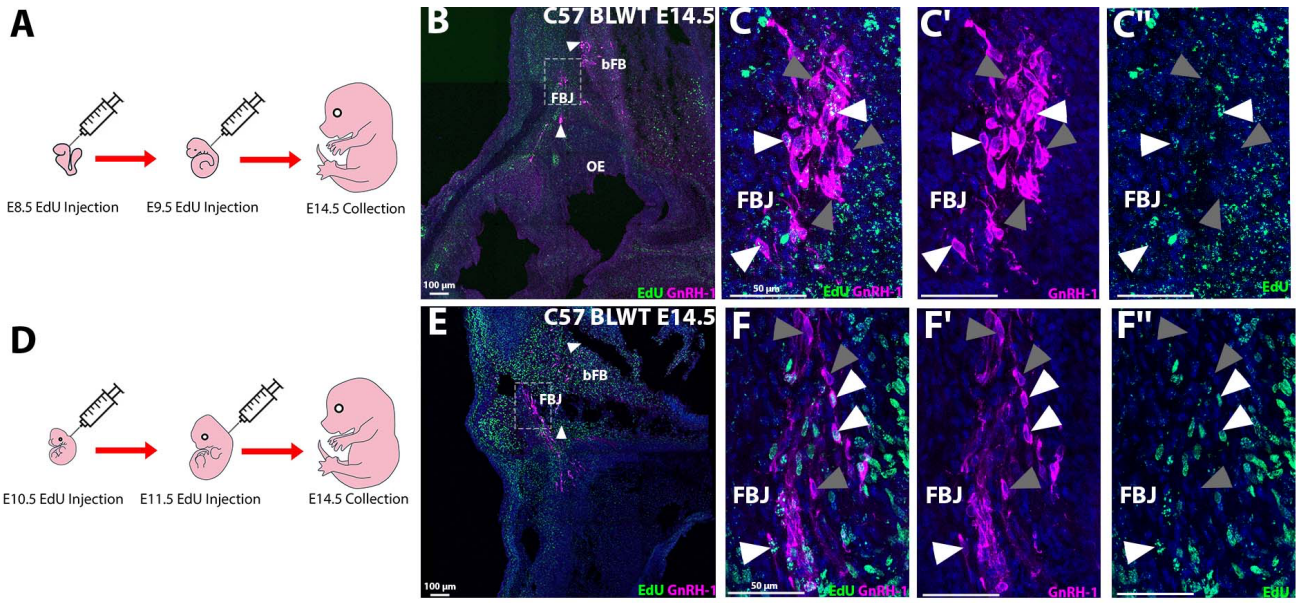

Figure S3.
GnRH-1 EdU Birth-dating Experiments.
A) Schematic of E8.5 and E9.5 EdU injection experiments, then collection at E14.5. B-C'') E14.5 C57 BLWT control tissue immunostained for EdU (green) and GnRH-1 (magenta, grey arrowheads). D) Schematic of E10.5 and E11.5 EdU injection experiments, then collection at E14.5. E-F'') EdU labelling at E10.5 and E11.5 was abundant in the forebrain junction (FBJ) and basal forebrain (bFB), overlapping with GnRH-1 immunoreactivity (white arrowheads). Scale bars in B, E 100 µm; C-C'', F-F'', 50 µm.

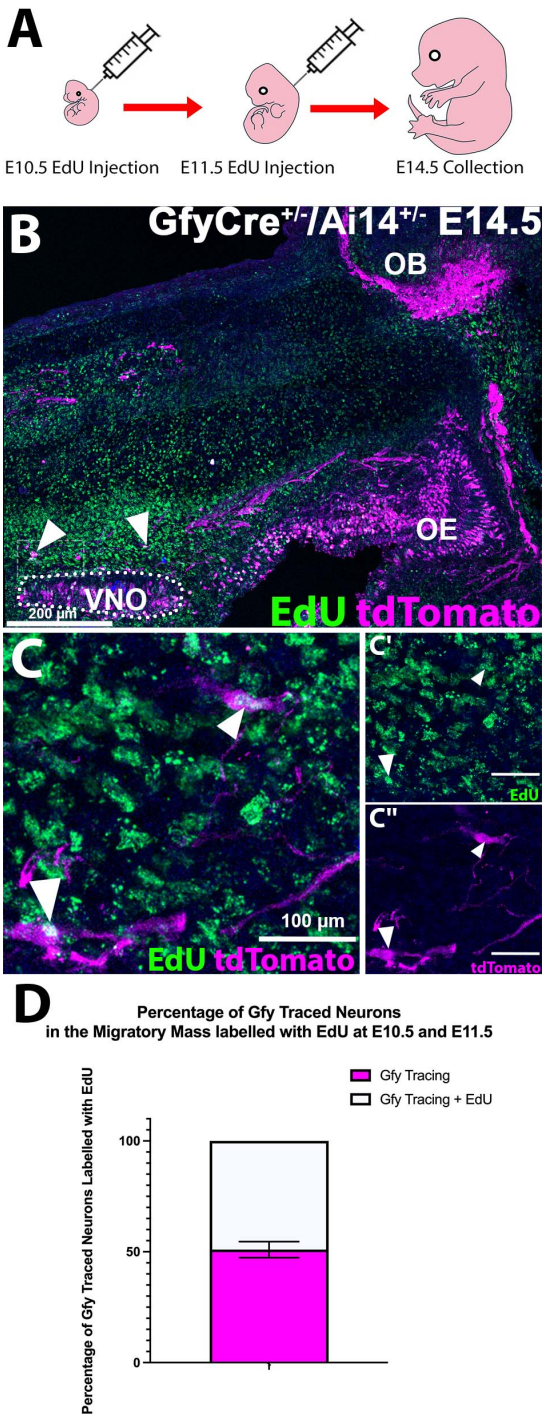

Figure S4.

Gfy Tracing EdU Brith-dating Experiments in Migratory Mass.

A) Schematic of EdU injection experiments performed at E10.5 and E11.5 and subsequently collected at E14.5. B) Parasagittal section on E14.5 GfyCre$^{+/-}$ /Ai14$^{+/-}$ embryos stained for EdU (green) and Gfy tracing (magenta). C-C'') Gfy tracing (magenta) and EdU staining (green) overlap (white) indicated with the arrowheads. D) Quantifications of EdU positive Gfy traced migratory neurons in the migratory mass. Scale bars in B, 200 µm; C-C'', 100 µm.

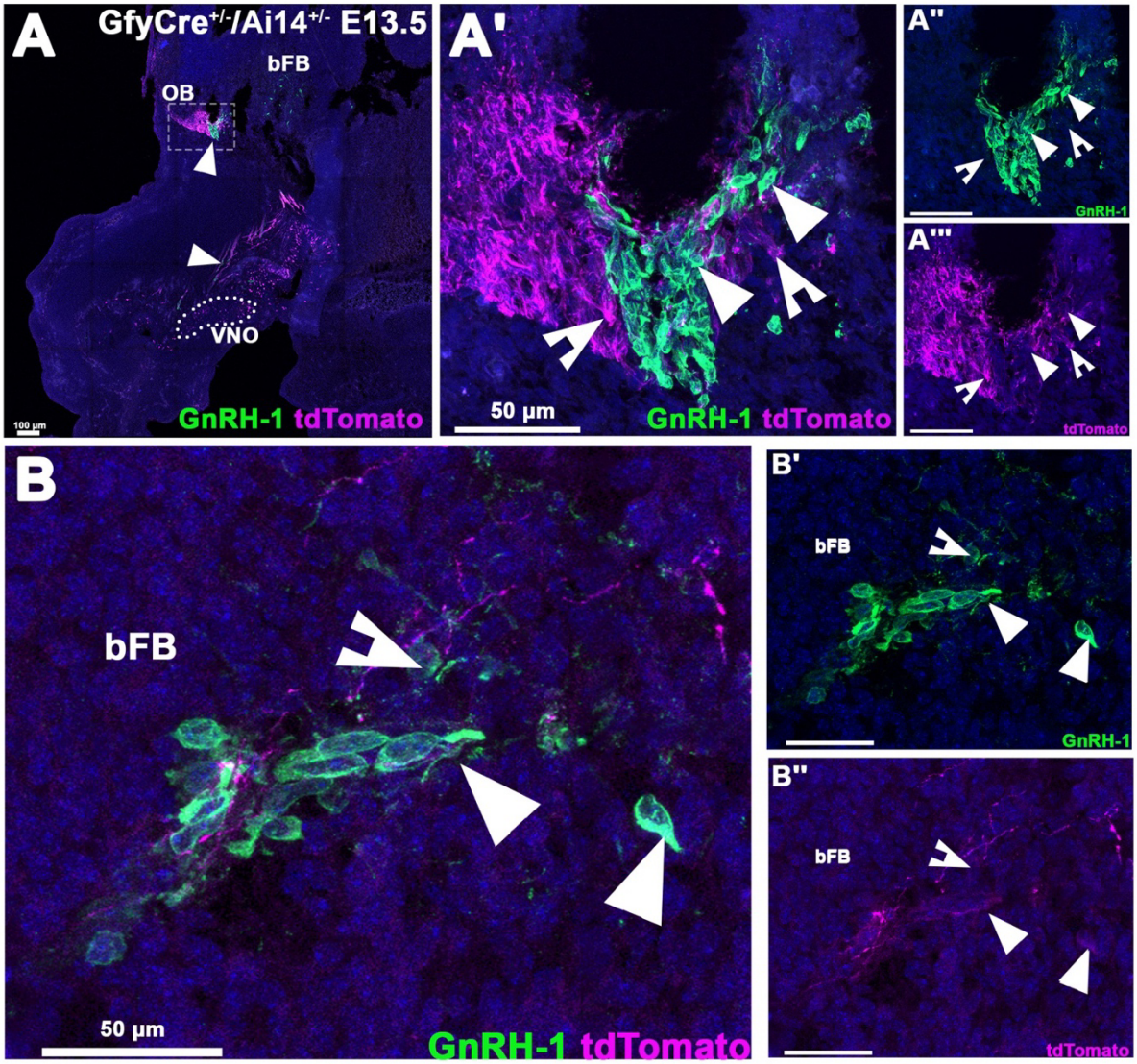

Figure S5.

The GnRH-1 neurons are closely intertwined with Gfy traced fibers in the brain.

A-A'') E13.5 GfyCre$^{+/-}$/Ai14$^{+/-}$ sections paired with GnRH-1 immunofluorescent staining. At this stage, GnRH-1 neurons (green, arrowheads) are migrating out of the vomeronasal organ (VNO), surrounded by Gfy traced cell bodies and axons/fibers (magenta, notched arrowheads) that also appear to be migrating out of the VNO. The GnRH-1 neurons invading the brain are not traced for Gfy. B-B'') GnRH-1 neurons invading the basal forebrain (bFB) with faint Gfy traced fibers entangling the GnRH-1 neurons and some Gfy traced cell bodies entering the brain. Scale bars in A, 100 µm; B-B'', C-C'', 50 µm.

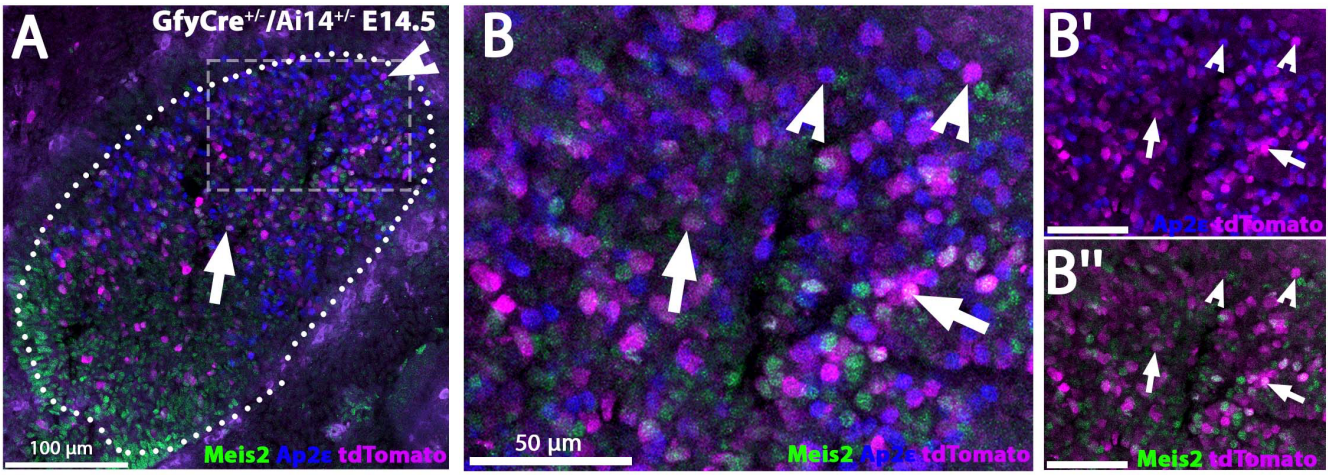

Figure S6. Genetic lineage tracing of Gfy in the embryonic VNO.
A-B'') E14.5 GfyCre$^{+/-}$/Ai14$^{+/-}$ vomeronasal organ (VNO) sections stained for vomeronasal sensory neuron (VSN) populations, Meis2 (green, arrows, apical) and AP-2ε (blue, notched arrowheads, basal). Both apical and basal developing VSNs were positive for Gfy tracing at E14.5. Scale bars in A, 100 µm; B-B'', 50 µm.

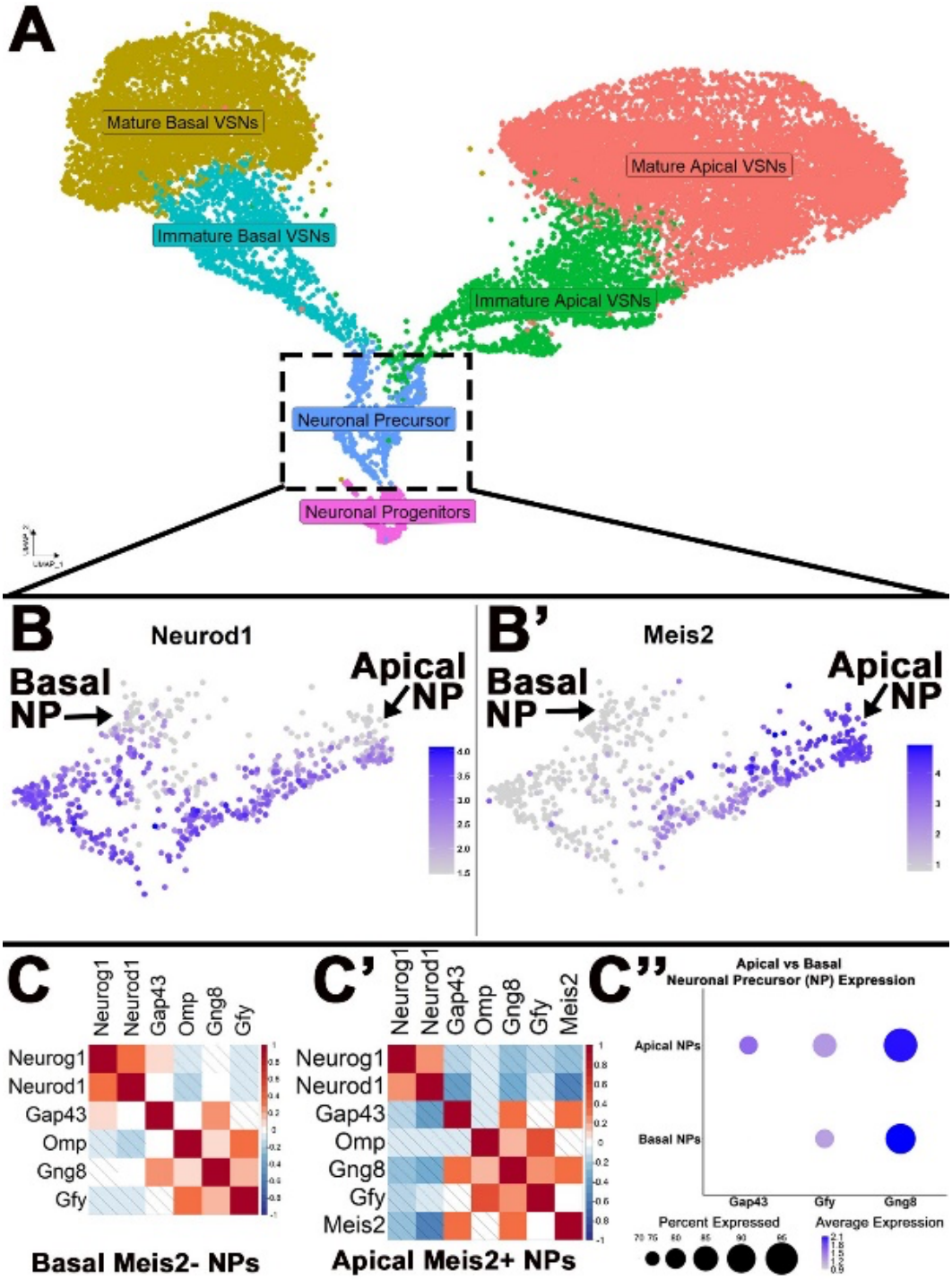
A
Mature Basal VSNs
Mature Apical VSNs
Immature Basal VSNs
Immature Apical VSNs
Neuronal Precursor
Neuronal Progenitors
B
Neurod1
Basal NP
Apical NP
B'
Meis2
Basal NP
Apical NP
C
Neurog1
Neurod1
Gap43
Omp
Gng8
Gfy
Basal Meis2- NPs
C'
Neurog1
Neurod1
Gap43
Omp
Gng8
Gfy
Meis2
Apical Meis2+ NPs
C''
Apical vs Basal
Neuronal Precursor (NP) Expression
Apical NPs
Basal NPs
Gap43
Gfy
Gng8
Percent Expressed
Average Expression

1007 **Figure S7. Single-cell transcriptomic analysis of the postnatal vomeronasal organ**
1008 **neuronal precursor populations.**
1009 A) UMAP projection of scRNA-seq data from the postnatal vomeronasal organ illustrating
1010 the major neuronal populations: the Neuronal Progenitors, Neuronal Precursors, immature
1011 apical and basal VSNs, and mature V1R/Meis2+ and V2R/AP-2ε+ VSNs. B-B') UMAP feature
1012 plots of the neuronal precursor population, Neurod1 highlights both apical and basal
1013 neuronal precursors (NP), while Meis2 expression is more enriched in apical neuronal
1014 precursors. C-C') Correlation matrix showing correlations between the neuronal precursor
1015 markers Neurod1 and key maturation markers (Gap43, Gng8, Gfy, Meis2). C'') Dotplot
1016 illustrating the expression pattern of Gap43, Gfy and Gng8 across both the apical basal
1017 populations of neuronal precursors.

1018